

MESTRADO  
MEDICINA LEGAL

# **Crosstalk between autophagic intermediaries in neurotoxicity induced by Synthetic Cannabinoids**

Catarina Pereira Teixeira

**M**  
2021

**U. PORTO**



**U. PORTO**

**Catarina Pereira Teixeira.** Crosstalk between autophagic intermediaries in neurotoxicity induced by Synthetic Cannabinoids



**M.ICBAS 2021**

**Crosstalk between autophagic intermediaries in neurotoxicity induced by Synthetic Cannabinoids**

Catarina Pereira Teixeira

INSTITUTO DE CIÊNCIAS BIOMÉDICAS ABEL SALAZAR



Catarina Pereira Teixeira

## **Crosstalk between autophagic intermediaries in neurotoxicity induced by Synthetic Cannabinoids**

Dissertation for the master's degree in Legal Medicine submitted to the Abel Salazar Institute of Biomedical Sciences (ICBAS) from the University of Porto.

**Supervisor:** Dr Diana Dias da Silva

**Category:** Investigator & Invited Auxiliary Professor

**Affiliations:** Associate Laboratory i4HB – Institute for Health and Bioeconomy, UCIBIO – Applied Molecular Biosciences Unit, REQUIMTE Laboratory of Toxicology, Department of Biological Sciences, Faculty of Pharmacy, University of Porto & TOXRUN – Toxicology Research Unit, Department of Sciences, University Institute of Health Sciences (IUCS), CESPU

**Co-Supervisor:** Dr João Pedro Silva

**Category:** Investigator

**Affiliation:** Associate Laboratory i4HB – Institute for Health and Bioeconomy, UCIBIO – Applied Molecular Biosciences Unit, REQUIMTE Laboratory of Toxicology, Department of Biological Sciences, Faculty of Pharmacy, University of Porto

**Co-Supervisor:** Dr Maria José Pinto da Costa

**Category:** Invited Associate Professor

**Affiliation:** Institute of Biomedical Sciences Abel Salazar (ICBAS), University of Porto

The experimental work was carried out at the UCIBIO, REQUIMTE Laboratory of Toxicology, Faculty of Pharmacy, University of Porto.

This work was funded by FEDER – *Fundo Europeu de Desenvolvimento Regional* funds through the COMPETE 2020 – Operational Programme for Competitiveness and Internationalization (POCI), and by Portuguese funds through FCT – *Fundação para a Ciência e a Tecnologia* in the framework of the project **POCI-01-0145-FEDER-029584**, as well as by the Applied Molecular Biosciences Unit (UCIBIO), funded by FCT through the grant with reference UIDB/04378/2021.

Cofinanciado por:





## ACKNOWLEDGMENTS

I would first like to thank the Laboratory of Toxicology of Faculty of Farmacy for giving me the opportunity to work in there and for providing me the necessary conditions for the elaboration of this dissertation.

My biggest thank is to Dr Diana Dias da Silva, my thesis advisor, for all the guidance and for making me feel at ease working in the lab, and most of all, for always having an open door when I needed. Her support and criticism have been imperative for the development of this work. Thank you for everything you taught me, but mostly, for always having a smile on your face. I would also like to thank Dr João Pedro Silva, for his availability and precious advice, it was a pleasure to have you as my co-advisor. Thank both for making me a better scientist, and most of all, for believing in me. To Dr Maria José Pinto da Costa for all the words, support, and knowledge you transmitted me in these years.

A big acknowledgment to all the TOXI group, particularly to Cátia and Margarida, the most amazing workers in the lab, their support has been essential from the start. I couldn't have done this without your help. Rita and Rafaela, there are no words to express how much you meant for my personal and professional growth. Rita, you are the most patient person, you were always ready to assist me, words aren't enough to thank you and your support. Rafaela, for being my friend at every hour, and for listening my drama and helping me with them, thank you, my friend. I must also thank Sandra, for all the laughs, help and company.

Ana and Catarina, thanks for your support all these years, you are the best master fellows I could ask for.

To my family and friends, thank you for dealing with me for the past 25 years, you were my great pillar in this journey. A special thank you to my mom, who always made sure I had everything I could wish for and more, and my father for all the positivity. You made me what I am today.

To David, a special thank you, even far away, always present.

To all of you, I will be eternally grateful, hope to make you all proud.



## ABSTRACT

Synthetic Cannabinoids (SCs) comprise a chemically heterogeneous group of new psychoactive substances (NPSs) that have gained popularity as drugs of abuse over the past decades, and are frequently involved in fatal and non-fatal intoxications. SCs currently represent the largest group of NPSs monitored by the European Monitoring Centre for Drugs and Drug Addiction. These molecules bind and activate cannabinoid receptors (CBRs), being potent agonists of CB1R and/or CB2R and eliciting cannabimimetic effects usually higher than those of *trans*- $\Delta^9$ -tetrahydrocannabinol ( $\Delta^9$ -THC).

Autophagy is a lysosome-dependent intracellular degradation pathway required for various physiological processes, which plays a housekeeping role in removing misfolded or aggregated proteins and clearing damaged organelles. Stimulation of autophagy by exogenous cannabinoids, in particular SCs, is not fully understood, with the majority of the studies presenting conflicting results. Our group recently showed that SCs are able to increase autophagy levels, as indicated by the higher number of autophagosomes in NG108-15 neuroblastoma x glioma hybrid cells following exposure to a set of structurally different SCs for 24h. This work thus aimed at assessing the mechanisms underlying such SC-induced autophagy in the same neuronal cell model.

The alteration in the levels of certain proteins involved in autophagy was analysed in NG108-15 cells after 24-h exposure to each SC at 1 nM and/or 1  $\mu$ M. In particular, the expression of ATG5, Beclin-1, Rab7A, LC3, and ubiquitin, following exposure to SCs was analysed using Western blot.

The results showed no statistically significant differences in the expression of the autophagy markers analysed. However, this could be possibly related to the high variability in the data obtained and the reduced number of independent experiments performed, since changes in protein expression relatively to the solvent control were observed, although with high associated standard deviations. For example, we observed higher expression levels of the autophagic related protein 5, ATG5, for all tested SCs, and all except AB-CHMINACA and 5F-AMB, tended to increase Beclin-1 expression, compared to the solvent control. Moreover, AB-FUBINACA (1  $\mu$ M), AB-PINACA (1 nM), AB-CHMINACA (1 nM) and SDB-006 (1  $\mu$ M) showed a slight increase in the autophagy intermediary Rab7A expression, over the control. All SCs, except AMB-FUBINACA (1 nM), AB-FUBINACA (1  $\mu$ M) and JWH-122 (1  $\mu$ M) showed an increasing trend in LC3 expression.

In summary, to help elucidate the toxicological effects of SCs and, in particular, to better understand how these substances increase autophagy, further research is required



to peremptorily conclude on the involvement of ATG5, Beclin-1, Rab7A, LC3, and ubiquitin on such processes.

**Keywords:** Cannabinoids; Autophagy; Beclin-1; ATG5; LC3; Rab7A; Ubiquitin.

## RESUMO

Os canabinóides sintéticos (CSs) compreendem um grupo quimicamente heterogêneo de novas substâncias psicoativas (NSPs) que ganharam popularidade como drogas de abuso, na última década, e estão frequentemente envolvidas em intoxicações fatais e não-fatais. Os CSs representam atualmente o maior grupo de NSPs monitorizadas pelo Observatório Europeu da Droga e da Toxicodependência. Estas moléculas ligam-se e ativam recetores canabinóides (RCBs), sendo potentes agonistas do RCB1 e/ou RCB2, e induzindo efeitos canabimiméticos habitualmente superiores aos do *trans*- $\Delta^9$ -tetrahydrocannabinol ( $\Delta^9$ -THC).

A autofagia é uma via de degradação intracelular dependente do lisossoma, necessária para vários processos fisiológicos e que desempenha um papel de remoção de proteínas disfuncionais e de eliminação de organelos danificados. A indução da autofagia por canabinóides exógenos, em particular por CSs, não é totalmente compreendida, já que a maioria dos estudos apresenta resultados controversos. Recentemente, o nosso grupo demonstrou que os CSs são capazes de aumentar os níveis de autofagia, tal como indicado pelo aumento do número de autofagossomas em células NG108-15 híbridas de neuroblastoma x glioma, após incubação com um conjunto de CSs estruturalmente diferentes, durante 24h. Desta forma, este trabalho teve como objetivo avaliar os mecanismos subjacentes à autofagia induzida por CSs no referido modelo de células neuronais.

A alteração nos níveis de certas proteínas envolvidas na autofagia foi analisada em células NG108-15 após exposição a cada CS a 1 nM e/ou 1  $\mu$ M, durante 24h. Em particular, a expressão de ATG5, Beclina-1, Rab7A, LC3 e ubiquitina foi analisada por Western-Blot, após exposição aos CSs.

Os resultados mostraram a ausência de diferenças estatisticamente significativas na expressão dos mediadores autofágicos testados. Contudo, isto poderá estar relacionado com a elevada variabilidade dos resultados obtidos e com o reduzido número de experiências independentes, uma vez que se observaram diferenças na expressão das proteínas relativamente ao controlo de solvente, mas com grandes desvios padrão associados. Por exemplo, para todos os CS, observámos elevados níveis de expressão da proteína relacionada com autofagia 5, ATG5, e, com exceção do AB-CHMINACA e do 5F-AMB, todos levaram a um aumento da expressão da Beclina-1, em comparação com o

grupo controlo. Além disso, verificou-se um pequeno aumento na expressão do mediador autofágico Rab7A para o AB-FUBINACA (1  $\mu$ M), AB-PINACA (1 nM), AB-CHMINACA (1 nM) e SDB-006 (1  $\mu$ M), relativamente ao controlo. Todos os CSs, exceto o AMB-FUBINACA (1 nM), AB-FUBINACA (1  $\mu$ M) e JWH-122 (1  $\mu$ M) mostraram um aumento da expressão de LC3.

Concluindo, para auxiliar na elucidação dos efeitos toxicológicos destes CS e, em particular, para melhor compreender como estas substâncias aumentam os níveis de autofagia, é necessária investigação adicional para taxativamente poder inferir sobre o envolvimento do ATG5, Beclin-1, Rab7A, LC3 e da ubiquitina nestes processos.

**Palavras-Chave:** Canabinoides; Autofagia; Beclin-1; ATG5, LC3; Rab7A; Ubiquitina.

## TABLE OF CONTENTS

<b>ACKNOWLEDGMENTS</b> .....	<b>v</b>
<b>ABSTRACT</b> .....	<b>vii</b>
<b>RESUMO</b> .....	<b>ix</b>
<b>FIGURES INDEX</b> .....	<b>xiii</b>
<b>ABBREVIATION LIST</b> .....	<b>xiv</b>
<b>1. INTRODUCTION</b> .....	<b>1</b>
1.1. Autophagy.....	1
1.2. Cannabinoids.....	5
1.2.1 Synthetic Cannabinoids (SCs) .....	7
1.3. SCs-mediated autophagy.....	7
<b>2.AIMS</b> .....	<b>10</b>
<b>3. MATERIALS AND METHODS</b> .....	<b>11</b>
3.1. Reagents .....	11
3.2 Cell culture.....	12
3.2.1 Hybrid somatic cell line NG108-15.....	12
3.2.2 Maintenance of cell cultures.....	12
3.2.3 Cell seeding.....	12
3.2.4 Exposure to SCs.....	13
3.3 Expression of autophagy intermediates by Western Blot.....	13
3.3.1 Total protein extraction and quantification .....	13
3.3.2 Western-Blotting.....	13
3.4 Statistical analysis .....	17
<b>4. RESULTS AND DISCUSSION</b> .....	<b>18</b>
4.1 Alterations on autophagic mediators.....	18

4.1.1 Alterations on autophagic mediator Beclin-1 .....	18
4.1.2 Alterations on autophagic mediator ATG5.....	20
4.1.3 Alterations on autophagic mediator LC3.....	22
4.1.4 Alterations on autophagic mediator Rab7A .....	26
4.1.5 Alterations on autophagic mediator ubiquitin.....	28
<b>5. CONCLUSIONS .....</b>	<b>29</b>
<b>6. REFERENCES .....</b>	<b>30</b>
<b>7. APPENDIXES .....</b>	<b>35</b>
I. Graphs of the different experiences for Beclin-1 .....	35
II. Graphs of the different experiences for ATG5.....	37
III. Graphs of the different experiences for LC3.....	39
IV. Graphs of the different experiences for Rab7A.....	40

## FIGURES INDEX

Figure 1. The three types of autophagy. ....	2
Figure 2. The mechanisms involved in autophagy. ....	3
Figure 3. A schematic representation of the proposed mechanisms by which cannabinoids induce autophagy. ....	8
Figure 4. Chemical structure of the SCs tested. ....	11
Figure 5. Expression of autophagic intermediary Beclin-1, in response to SCs, as assessed by Western-Blot. ....	19
Figure 6. Expression of autophagic intermediary ATG5, in response to SCs, as assessed by Western-Blot. ....	21
Figure 7. Expression of autophagic intermediary LC3, in response to SCs, as assessed by Western-Blot. ....	23
Figure 8. Expression of autophagic intermediary Rab7A, in response to SCs, as assessed by Western-Blot. ....	27
Figure 9. Expression of autophagic intermediary ubiquitin, in response to SCs, as assessed by Western-Blot. ....	28

## ABBREVIATION LIST

2-AG – 2-Arachidonoylglycerol

$\Delta^9$ -THC – *trans*- $\Delta^9$ -Tetrahydrocannabinol

AEA – Anandamide

AKT – Protein kinase B

AMPK – Adenosine monophosphate activated protein kinase

ATF4 – Activating transcription factor 4

ATG – Autophagy related protein

Bcl-2 – B-Cell lymphoma 2

BSA – Bovine serum albumin

CB1R – Cannabinoid receptor 1

CB2R – Cannabinoid receptor 2

CBD – Cannabidiol

CHOP – CCAAT/Enhancer-binding protein homologous protein

CMA – Chaperone-mediated autophagy

DMEM – Dulbecco's modified Eagle's medium

DMSO – Dimethyl sulfoxide

DTT – Dithiothreitol

ECS – Endocannabinoid system

EMCDDA – European Monitoring Centre for Drugs and Drug Addiction

ER – Endoplasmic reticulum

FBS – Fetal bovine serum

FIP 200 – Family interacting protein 200

GPCR – G Protein-coupled receptor

LAMP-2A – Lysosomal-associated membrane protein 2A

LC3 – Microtubule-associated protein 1A/1B-light chain

mTOR – Mammalian target of rapamycin

NPS – Novel psychoactive substance

p8 – Stress modulated protein p8

Pen-Strep – Penicillin-streptomycin

PI – Phosphatidylinositol

PI3P – Phosphatidyl inositol triphosphate

PVDF – Polyvinylidene difluoride

SC – Synthetic Cannabinoid

SDS – Sodium dodecyl sulphate

SDS-PAGE – Sodium dodecyl sulphate polyacrylamide gel electrophoresis

TBS – Tris-buffered saline

TBST – Tris-buffered saline with tween 20

TRB3 – Pseudokinase tribbles homologue 3

ULK1 – Unc-51-like kinase

VPS34 – Vesicular protein sorting 34



## 1. INTRODUCTION

### 1.1. Autophagy

The term “autophagy”, literally derived from the Greek “eating of self” [1] concerns a highly conserved cellular process in which, under stress conditions (e.g., nutrient deficit or drug treatment), cytoplasmic materials, including intracellular misfolded or long-lived proteins, superfluous or damaged organelles, and invading microorganisms, are sequestered into double-membrane vesicles called autophagosomes. These are further fused with lysosomes for degradation or recycling [2-4]. Such “self-digestion” usually provides cells with more nutrients for continuous survival. As such, the basic function of autophagy is to maintain cellular homeostasis [5].

Besides its role in cell survival, autophagy can also be a form of programmed cell death [2]. In this sense, autophagy may display very distinct roles in the onset and progression of different diseases. In some cases, autophagy shows an adaptive response to survival, whereas in other ones, deregulated autophagy is central to the pathogenesis of many human disorders such as neurodegenerative diseases, cancer, infectious diseases, heart failure, and diabetes [6].

Autophagy has recently gained attention among numerous research groups, which have contributed to the molecular understanding of the physiological significance of this process. There are three defined types of autophagy currently acknowledged: microautophagy, macroautophagy, and chaperone-mediated autophagy (CMA), all of which promote proteolytic degradation of cytosolic components in the lysosome [1]. These are summarized in **Fig. 1**. The difference between micro- and macroautophagy lies in the transport of the material to be degraded, the type of transported material and its regulation [7]. Microautophagy has been traditionally considered as a form of active autophagy to ensure the turnover of long-lived proteins under basal conditions [1]. During microautophagy, the lysosomes incorporate and digest portions of cytosol, including proteins and cytoplasmic organelles, by invagination or protrusion of the lysosomal membrane without the intermediate formation of autophagic vacuoles [7]. In contrast, macroautophagy, hereafter referred as autophagy, delivers cytoplasmic material to the lysosome through the intermediary of a double-membrane vesicle, called autophagosome, whose external membrane fuses with the lysosome to form an autophagolysosome where the cytosolic compartments and internal membrane are degraded. Thus, both macro- and

microautophagy comprise the engulfment of large structures through both selective and non-selective mechanisms [1].

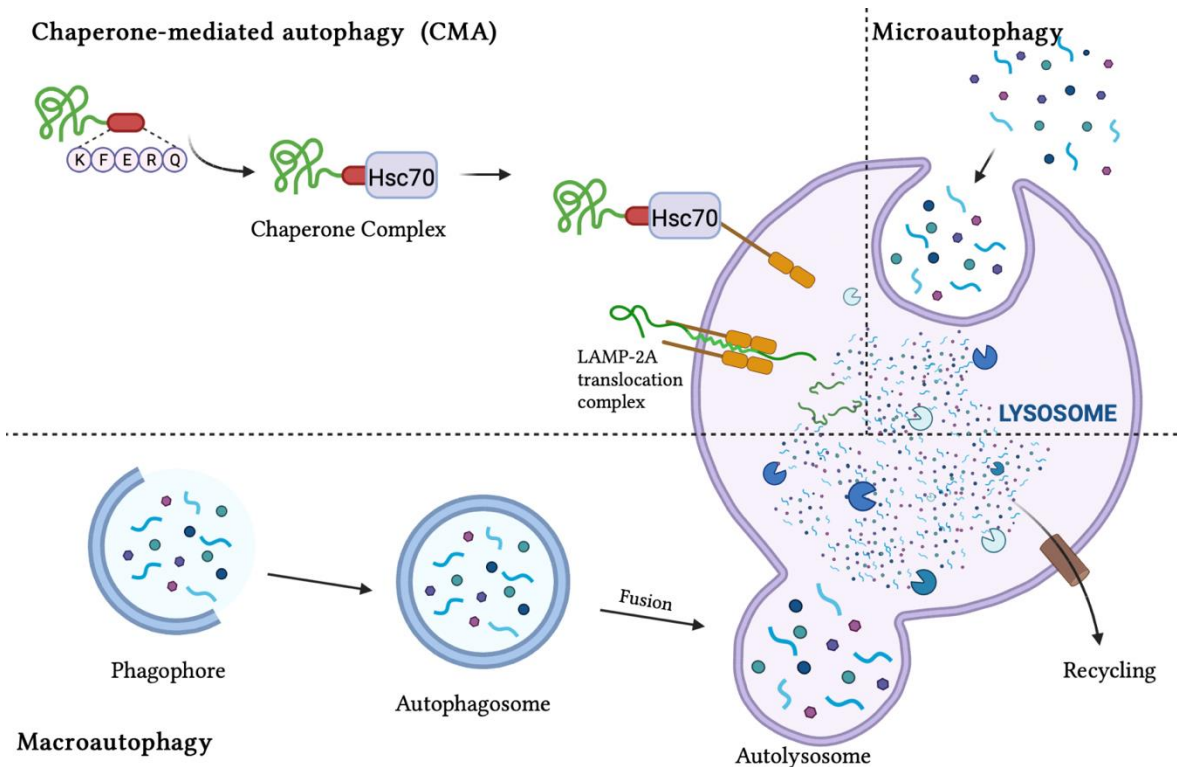


**Figure 1.** The three types of autophagy. In CMA, individual unfolded proteins are transported directly across the lysosomal membrane; In Microautophagy the lysosomes incorporate and digest portions of cytosol by invagination or protrusion of the lysosomal membrane; Macroautophagy relies on formation of autophagosomes, cytosolic double-membrane vesicles that transport cargo to the lysosome. Created in BioRender.com.

In CMA, the targeted proteins, combined with a KFERQ motif (a peptide motif), are bound in a complex with chaperone proteins (such as Hsc70) and recognized by the lysosomal membrane receptor lysosomal-associated membrane protein 2A (LAMP-2A), resulting in their unfolding and degradation [1, 8].

In particular, the intricacy of autophagy can be abridged in five key stages: initiation, nucleation, elongation, maturation, and fusion [9]. The process initiates with the formation of a phagophore, consisting of an isolation membrane that, accordingly to current understanding, involves activation of the Unc-51-Like Kinase 1 (ULK1) complex (**Fig. 2**),

composed of four factors, including ULK1, autophagy related gene (ATG)13, focal adhesion kinase family interacting protein 200 (FIP 200), and ATG101 [1, 10, 11].

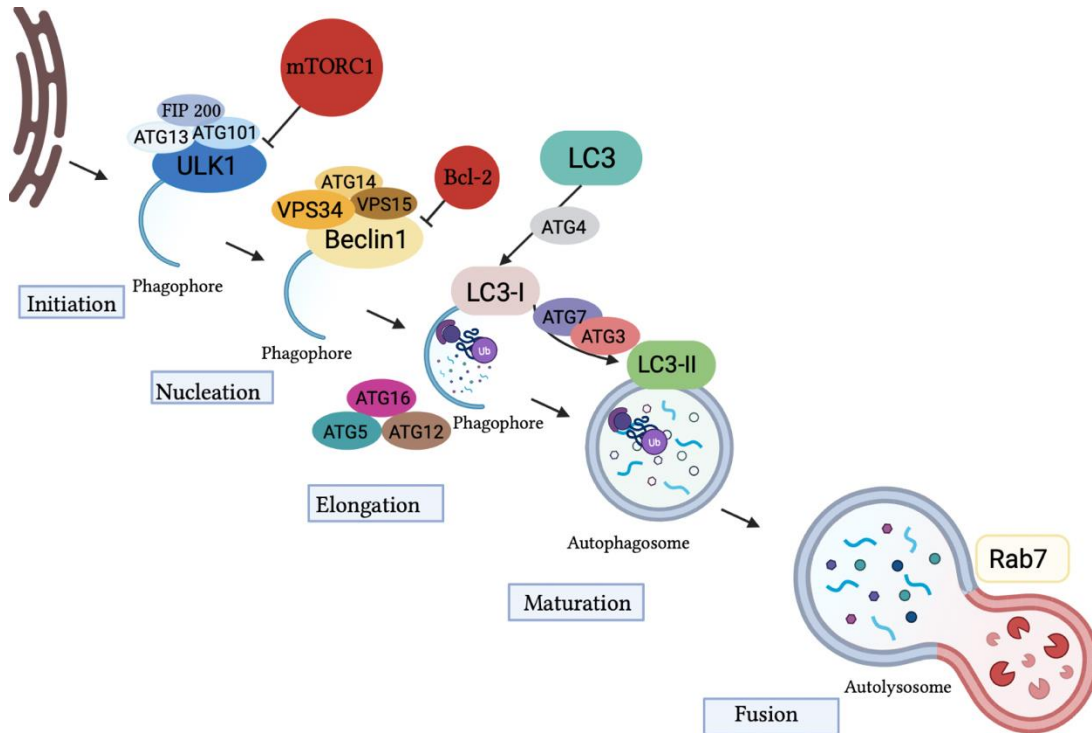


**Figure 2.** The mechanisms involved in autophagy. The initiation requires the complex ULK1-ATG13-FIP 200-ATG101, activated by mTORC1 inhibition. To nucleation process Beclin1- VSP15-VSP34-ATG14 complex is required. So that the elongation of the phagophore occurs two systems are needed, the complex ATG5-ATG16-ATG12 and the second is LC3, which is converted by ATG4 to LC3-I and further to LC3-II so the maturation stage can happen. In the last stage the autophagosome fuses with lysosome, forming the autolysosome, with the Rab7A assistance. The autophagic cargo is degraded and recycle back to the cytosol. Created in BioRender.com.

The most characterised stimulus for induction of autophagy is the deprivation of amino acids, which results in inhibition of the master cell growth regulator serine/threonine kinase, the mammalian target of rapamycin – mTOR [9, 10]. mTOR is found in two distinct protein complexes, mTORC1 and mTORC2, but only mTORC1 directly regulates autophagy [12].

When nutrients and energy are sufficient, mTORC1 inhibits autophagy through direct phosphorylation of ULK1 and ATG13, inhibiting the formation of the autophagy-induction complex, the ULK1 complex [13, 14]. However, under starvation conditions, the activity of mTORC1 is inhibited, leading to autophagy-induced cell death. The key regulators of mTORC1 are AKT and adenosine monophosphate-activated protein kinase (AMPK). In the presence of growth factors, AKT is activated and activated AKT further activates mTORC1, inhibiting autophagy. In contrast, the decreased cellular energy status enhances the phosphorylation and activation of AMPK, which in turn suppresses mTORC1 activity, leading to autophagy. Under glucose starvation, AMPK activates ULK1 via phosphorylation of Ser317 and Ser777 residues, promoting autophagy. Under nutrient sufficiency, active mTORC1 prevents ULK1 activation by phosphorylating ULK1 at Ser757 site and disrupting the interaction between ULK1 and AMPK [14].

The required proteins to the phagophore nucleation are PI3Kinases (PI3K)-Class III, notably the vesicular protein sorting 34 (VPS4) and Beclin-1. VPS4 uses phosphatidylinositol (PI) as its substrate to generate phosphatidylinositol triphosphate (PI3P), which is essential for the recruitment of other ATG proteins to the phagophore complex. The interaction of Beclin-1 with VPS4 promotes its catalytic activity and increases levels of PI3P [1]. The Beclin-1 activity in autophagy is regulated through the apoptosis regulator B-cell lymphoma 2 (Bcl-2) [15]. Beclin-1 interacts with Bcl-2 to inhibit the formation of the Beclin-1/PI3K III complex, a mechanism that prevents the activation of autophagy. On the other hand, under starvation and other physiologic stimuli (*i.e.*, hypoxia), the dissociation of Bcl-2 from Beclin-1 activates autophagy [1, 15].

Ubiquitin is a highly conserved 76 amino acid globular protein that attaches to protein substrates via covalent conjugation (ubiquitination). Ubiquitination is implicated in multiple aspects of autophagy, the major lysosome/vacuole-dependent degradation pathway. Ubiquitin chains that are attached as labels to protein aggregates or subcellular organelles confer selectivity, allowing autophagy receptors to simultaneously bind ubiquitinated cargos and autophagy-specific ubiquitin-like modifiers [16, 17].

There are two ubiquitin-like systems that are preponderant to autophagy and act at the ATG5–ATG12 conjugation step and at the microtubule-associated protein 1A/1B-light chain 3 (LC3) processing step. In the first system, *i.e.*, ATG5–ATG12–ATG16, Atg7 acting like an E1 ubiquitin activating enzyme, activates Atg12 in an ATP-dependent manner by

binding to its carboxyterminal glycine residue. Then, Atg12 is transferred to Atg10, an E2-like ubiquitin carrier protein that facilitates covalent linkage of Atg12 to lysine 130 of Atg5. This leads to Atg5–Atg12 conjugation with Atg16L dimers to form a multimeric ATG5–ATG12–ATG16 complex essential to the extension/elongation of the phagophore [1].

The second ubiquitin-like system that is important for the formation and maturation of the autophagosome is LC3 [11]. LC3 is cleaved at its c-terminal by the protease ATG4 to form LC3-I [1]. Then, LC3 lipidation is orchestrated by ATG7, ATG3, and the complex ATG12-ATG5-ATG16, resulting in the conversion of LC3-I to LC3-II by conjugating the cytosolic LC3-I protein to phosphatidylethanolamine [18].

It is important to highlight that LC3-II is currently the only reliable marker of autophagosomes (starting from phagophore membrane to lysosomal degradation), the amount of LC3-II correlating well to the number of autophagosomes [19]. For that, LC3-II has become the most universally used marker for the detection of autophagy [9]. Taken together, this has made LC3-II a hallmark feature in studying the autophagic process.

Autophagosome formation is completed by the extension and closure of the phagophore [11]. Thereafter, the mature autophagosome is labelled with the Ras-related protein Rab7A, a small GTPase that is an effective multifunctional regulator of autophagy and that participates in the fusion of the autophagosome with the lysosome to form the autophagolysosome or autolysosome [20, 21]. The hybrid organelle (autolysosome) allows the degradation of the autophagosome's content by lysosomal enzymes, the autophagic cargo being then recycled back to the cytosol to provide energy for cell growth [22].

## **1.2. Cannabinoids**

Cannabinoids can be divided into three groups according to their origin: phytocannabinoid, which are plant-derived chemicals; endocannabinoids, which are produced in the human body; and human-made cannabinoids that are synthesised in laboratories [23].

Phytocannabinoids are found mostly in *Cannabis sativa* (cannabis), which was introduced into Western medicine and widespread in the Americas in 1841. Cannabis-

based extracts, tinctures, cigarettes, and plasters produced by early prominent drug companies were indicated for a wide range of pathological conditions, many of which were related to pain [24]. The well-known phytocannabinoid *trans*- $\Delta^9$ -tetrahydrocannabinol ( $\Delta^9$ -THC) is a cannabinoid receptors partial agonist, while cannabidiol (CBD) displays high potency as an agonist of cannabinoid receptors [25].

The endocannabinoid system (ECS) was discovered following the discovery of the structure of the psychotropic phytocannabinoid  $\Delta^9$ -THC (which is also responsible for some of *C. sativa*'s psychoactivity). The ECS comprises lipid ligands (endocannabinoids), their receptors, including cannabinoid receptor type 1 (CB1R) and cannabinoid receptor type 2 (CB2R), and the enzymes involved in their biosynthesis and degradation [26].

Endocannabinoids are endogenous lipids that act on CB1R and CB2R. Four endocannabinoids have been characterised, namely arachidonoylglycerol ether, virodhamine, *N*-arachidonylethanolamine or anandamide (AEA), and 2-arachidonoylglycerol (2-AG) [27]. To date, AEA and 2-AG are the most studied and well characterised endocannabinoids [23].

The first identified receptor, the CB1R, is a G protein-coupled receptor (GPCR) that is most abundantly expressed in the brain and central nervous system. However, these receptors can also be found in several other organs (e.g., kidney, lungs, liver, heart). The CB2R, which is also a GPCR, was later identified by homology cloning and found to be highly expressed in the immune system, although it is also present in other organs as well, including in the brain (mostly at post-synaptic locations) [28].

The worldwide use of cannabis is common and according to the World Drug Report from the United Nations Office on Drugs and Crime, cannabis is the most used drug worldwide, being estimated that almost 4 % (range: 2.8–5.1%) of the global population aged 15–64 years used cannabis at least once in 2019, the equivalent to about 200 million people (range: 141 million–256 million) [29].

### 1.2.1 Synthetic Cannabinoids (SCs)

Synthetic Cannabinoids (SCs) are a class of novel psychoactive substances (NPS) that were originally developed in laboratory, in a research context, with the intention to search for compounds with potential therapeutic use [23, 30]. As soon as the ECS (including endocannabinoids) was discovered, other molecules that acted on it began to be synthesized, either with pharmacological purposes or as a tool for research. Most of them were abandoned by the pharmaceutical industry, due to their associated adverse effects. However, they have emerged as recreational drugs in the early 2000s, on the “legal highs” market, in products labelled “Spice” or “herbal incense” [23, 24, 31]. Nowadays, SCs represent the largest group of NPS monitored by the European Monitoring Centre for Drugs and Drug Addiction (EMCDDA) through the EU Early Warning System [32].

SCs became drugs of abuse of high prominence due to the biological properties that they share with  $\Delta^9$ -THC, the main psychoactive substance present in cannabis [33-35]. These drugs also act by activating the CB1R and CB2R, but they are characterized by the full agonism of CB1R and/or CB2R. Since  $\Delta^9$ -THC acts in these receptors as a partial agonist, this pharmacological difference between the classic and the emerging drugs might justify the greater potential of the SCs to induce severe intoxication in their consumers [36].

Although the SCs toxicity and toxicological mechanisms are not thoroughly documented, there is countless evidence of a considerable number of hospitalizations as a consequence of the acute exposure to these drugs, often culminating in severe or even fatal detrimental effects [36, 37]. The intoxication symptoms caused by SCs include anxiety, hallucinations, irritability, seizures, paranoia, psychosis, tachycardia/bradycardia, hypertension, myocardial infraction, arrhythmias, chest pain, and palpitations, the cardiovascular and central nervous systems being the main targets [31, 36, 38-40].

### 1.3. SCs-mediated autophagy

Stimulation or inhibition of autophagy by cannabinoids is controversial and not fully understood, yet cannabinoid-induced autophagy seems to mainly occur through activation of members of AMPK family or stimulation of *de novo* synthesis of ceramide [41, 42].

In some cases, cannabinoid administration produces Endoplasmic Reticulum (ER) stress and accumulation of *de novo*-synthesized ceramide in the ER, by inhibition of pseudokinase tribbles homologue 3 (TRB3). TRB3 promotes an inhibitory interaction of this protein with Akt, leading in turn to mTORC1 inhibition and consequent activation of autophagy [41, 42]. Also, the increase in eukaryotic translation initiation factor 2, subunit 1 alpha (eIF2 $\alpha$ ) phosphorylation, a factor required for the upregulation of stress modulated protein p8 (p8) as well as for induction of autophagy, upregulation of TRB3 and p8 (upregulated in response to ER stress activation) and its downstream targets, such as activating transcription factor 4 (ATF4), an important factor that induces expression of autophagy genes including LC3, ULK1 and ATG5 [43], CCAAT/enhancer-binding protein homologous protein (CHOP), a protein that promotes the transcription of autophagy genes through the cooperation with ATF4 [44], leads to inhibition of AKT/mTORC1 axis and subsequent autophagy activation (**Fig. 3**) [22, 41, 45]. Moreover, knockdown of p8 or TRB3 prevent cannabinoid (THC)-induced autophagy, proving its importance in cannabinoid-induced autophagy [41].

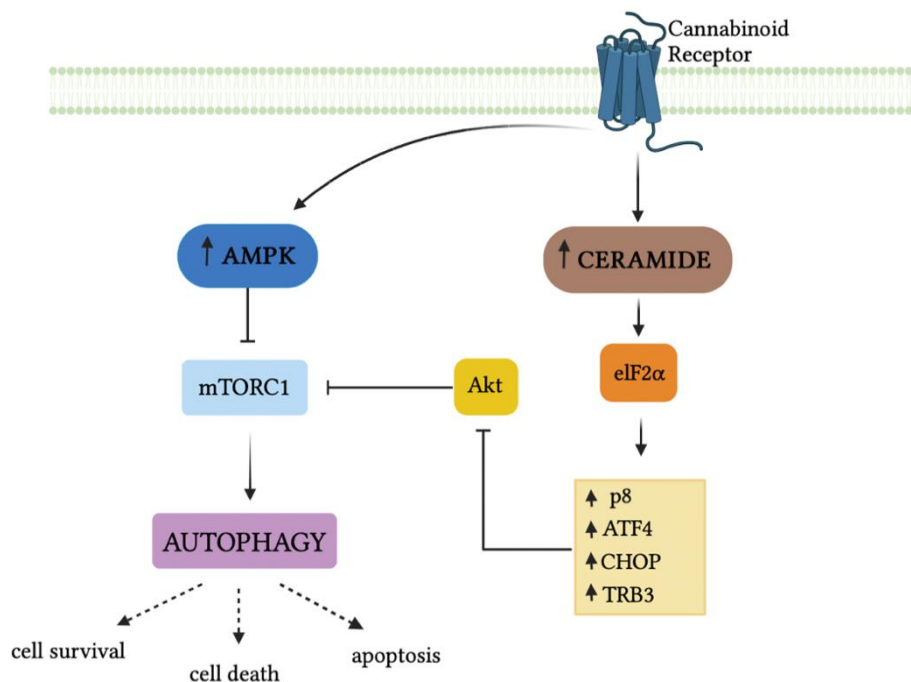


**Figure 3.** A schematic representation of the proposed mechanisms by which cannabinoids induce autophagy. Cannabinoid treatment can induce autophagy via two different mechanisms: activation of AMPK or stimulation of *de novo* synthesis of ceramide. Cannabinoid-induced autophagy may lead to cell survival, cell death or apoptosis. Created in BioRender.com.



In other cases, AMPK activation seems to be necessary for cannabinoids-induced autophagy. AMPK activation leads, subsequently to the inhibition of mTORC1, allowing autophagy to occur [42].

Salazar et al. (2009) observed that 6  $\mu\text{M}$   $\Delta^9$ -THC induced ER dilation in human glioma U87MG cells, as detected by immunostaining of the ER luminal marker protein disulphide isomerase. By using cells derived from eIF2 $\alpha$  S51A knock-in mice, the authors further found that  $\Delta^9$ -THC treatment upregulated p8, ATF4, CHOP and TRB3 by modulating the phosphorylation of eIF2 $\alpha$ , as determined by real-time quantitative PCR, proving  $\Delta^9$ -THC-induced autophagy via ER stress-dependent upregulation of p8 and TRB3 [41].

In agreement with these findings, Vara et al. (2011) have demonstrated that 8  $\mu\text{M}$   $\Delta^9$ -THC and JWH-015 treatment for 24h, in hepatocellular carcinoma HepG2 cells, and 24h treatment with 5  $\mu\text{M}$   $\Delta^9$ -THC and JWH-015, in in hepatocellular carcinoma HuH7 cells, upregulated TRB3, also, 8  $\mu\text{M}$  treatment of  $\Delta^9$ -THC and JWH-015 increased the phosphorylation of eIF2 $\alpha$ . Moreover, inhibition of AKT and increasing of AMPK was evidenced after the 24h treatment with 8  $\mu\text{M}$  of  $\Delta^9$ -THC and JWH-015 for HepG2 cells and 5  $\mu\text{M}$  of each one, for HuH7 cells. This results, showed a markedly reduced the viability of this cell line through induction of autophagy, mediated, by upregulation of TRB3 and subsequent inhibition of the AKT and AMPK stimulation [42].

In accordance, after treatment of colon cancer HT29 cells with 10  $\mu\text{M}$  WIN55,212-2 (an SC), Pellerito et al. (2014) showed that the levels of phosphorylated Akt decreased. After 36h of 10  $\mu\text{M}$  WIN55,212-2 treatment, the levels of TRIB3 and CHOP increased, in HT29, HCT 116 and Caco-2 cell lines, proving that this cannabinoid induced ER stress and activated the autophagic pathway [46].

## **2.AIMS**

This group has recently observed (unpublished data) the occurrence of autophagy, after 24 h exposure of these cells to 14 SCs at 1 nM and 1  $\mu$ M, using the CYTO-ID® Autophagy Detection kit through flow cytometry analysed in the NG108-15 cell line. The results showed that 11 out of the 14 tested SCs induced autophagy, at least at one of the concentrations tested.

So, the main goal of this work was to elucidate the mechanisms involved in SC-induced neurotoxicity, in particular to evaluate the impact of a set of 11 structurally different SCs in the deregulation of autophagy in a neuronal cell line, NG108-15, by analysing the expression of known autophagy mediator markers (e.g., LC3, Beclin-1, ATG5, Rab7A and ubiquitin) following NG108-15 cells exposure to the SCs.

### 3. MATERIALS AND METHODS

#### 3.1. Reagents

Cell culture reagents were obtained from GIBCO Invitrogen (Alfagene, Portugal) and all other reagents from Sigma-Aldrich (Portugal), unless stated otherwise.

The SCs, namely AMB-FUBINACA (also known as FUB-AMB and MMB-FUBINACA), AB-PINACA, MDMB-CHMICA, AB-CHMINACA, 5F-AMB (also known as 5F-MMB-PINACA and 5F-AMB-PINACA), AB-FUBINACA, FUBIMINA (also known as BZ-2201), X-PB-22F (also known as 5F-NPB22), 5F-PB22, SDB-006 and JWH-122 (**Fig. 4**), were obtained from TicTac Communications Ltd (UK). Stock solutions of SCs were prepared in dimethyl sulfoxide (DMSO, Merck) and stored at -20°C, being diluted extemporaneously on the day of the experiment.

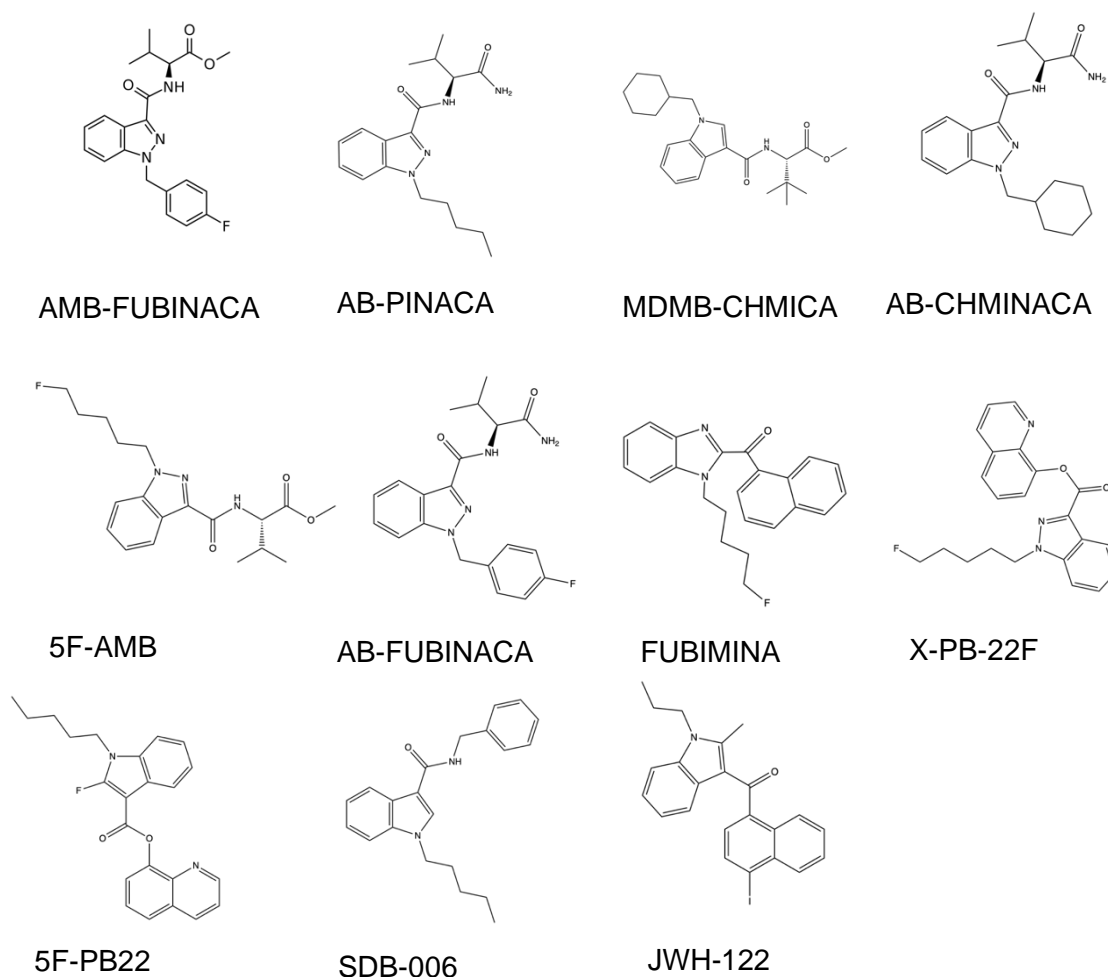


**Figure 4.** Chemical structure of the SCs tested.

## **3.2 Cell culture**

### **3.2.1 Hybrid somatic cell line NG108-15**

To meet the objectives of this project, the NG108-15 cell line was used. Initially called 108CC15, and developed in 1971 by Bernd Hamprecht, this cell line was obtained from the fusion of mouse (*mus musculus*) neuroblastoma cells (N18TG2) with glioma cells (C6-BU-1) of rat (*rattus norvegicus*) in the presence of inactivated Sendai virus. NG108-15 cells endogenously express CB1R and are often used in neurotoxicological studies as they are a well-characterized model of neuritogenesis and synapse formation from a blastoid state under stress conditions.

### **3.2.2 Maintenance of cell cultures**

The cell culture medium used was the Dulbecco's Modified Eagle's Medium (DMEM), high glucose, with phenol red (Sigma-Aldrich, Portugal) supplemented with 10% heat inactivated fetal bovine serum (FBS) and 1% PenStrep (penicillin-streptomycin solution, 10,000 U/mL). For the maintenance of cell culture, cells were observed daily, macroscopically and microscopically to assess their morphology, culture medium colour and cell density. The cells were cultured in 75 cm<sup>2</sup> flasks (Corning Life Science, USA), at 37°C under a humidified 5% CO<sub>2</sub> atmosphere, and subjected to regular medium changes (every two to three days) until reaching 70-80% confluence.

Whenever cells reached 80% confluence, they were sub-cultured (*i.e.*, passaged into new flasks, so they have more space to proliferate) by trypsinization with a 0.25% trypsin/EDTA solution, for no more than 10 passages.

### **3.2.3 Cell seeding**

After cell counting in a Neubauer chamber, the cells were seeded on 6-wells plates, at a density of 10<sup>6</sup> cells per well, in a volume of 2 mL of complete medium. They were left to adhere overnight at 37°C in a 5% CO<sub>2</sub> atmosphere, and exposed to the SCs on the next day.

### **3.2.4 Exposure to SCs**

For the evaluation of autophagy activation by Western blotting, cells were exposed to each SC, at concentrations of 1 nM and/or 1  $\mu$ M, and further incubated for 24 h at 37°C in a 5% CO<sub>2</sub> atmosphere. Positive control (i.e., starvation medium consisting of DMEM supplemented with 1% FBS and 1% PenStrep), negative control (only cell culture medium) and solvent control [cell culture medium with DMSO at the highest concentration tested; final DMSO concentration was always below 0.02%] were also included, in all cases. All treatments were tested in duplicate.

## **3.3 Expression of autophagy intermediates by Western Blot**

### **3.3.1 Total protein extraction and quantification**

The protein expression of specific mediators of autophagy was analysed by Western blotting in total protein extracts of NG108-15 cells exposed to SCs. Following the 24 h-incubation, cell culture medium was discarded; cells were scrapped in the presence of 1 mL of HBSS per well and collected into Eppendorf tubes. The cell suspensions were centrifuged at 11,000 g for 3 min at 4°C, and the supernatants discarded. The cells were resuspended in 40  $\mu$ L of lysis buffer (0.02 M Tris-HCl, 0.15 M NaCl, 0.005 M EDTA, 0.3% Triton X-100). The pellets were then disrupted by three sonication pulses of 10 sec intercalated with 10 sec on ice. The suspensions were, again, centrifuged at 11,000 g, for 5 min at 4°C; the supernatants were placed into new Eppendorf tubes.

Quantification of total protein in the cell extracts was performed using the Bio-Rad Detergent Compatible protein assay (Bio-Rad, Hercules, CA, USA), according to the manufacturer's instructions. The samples were then stored at -80°C until further use.

### **3.3.2 Western-Blotting**

#### **3.3.2.1 Sample preparation**

The samples were processed through a combination of biochemical and mechanical techniques. The amount of sample containing approximately 100  $\mu$ g of protein was denatured at 65°C for 3 min (to LC3) or 95°C (to Beclin-1, ATG5, Rab7A and ubiquitin), for 5 min, in 4x sample loading buffer [0.25 M Tris-HCl, 50% glycerol, 10% sodium dodecyl

sulphate (SDS), 0.2 M dithiotreitol (DTT) and 0.001% bromophenol blue], to promote cell lysis and solubilise proteins. Protease inhibitor cocktail, the phenylmethylsulfonyl fluoride (10 µL/mL; Sigma-Aldrich, Portugal) was added to prevent the proteolytic activity of the sample. Further sample handling was performed on ice to avoid protein denaturation and degradation.

### **3.3.2.2 Electrophoresis**

The proteins in the samples were separated using SDS-PAGE (SDS polyacrylamide gel electrophoresis) at 10% acrylamide for Beclin-1, 15% for ATG5, LC3 and Rab7A and 20% for ubiquitin. SDS-PAGE maintains polypeptides in a denatured stage once they have been treated with strong reducing agents, like SDS, to remove secondary and tertiary structure, and thus allowing separation of proteins by their molecular weight. Sample proteins become covered by the negatively charged SDS and move to the positively charged electrode through the acrylamide mesh of the gel. Smaller proteins migrate faster and are thus separated according to size (measured in kDa). The concentration of acrylamide determines the resolution of the gel – the greater the acrylamide concentration, the better the resolution of lower molecular weight proteins. The lower the acrylamide concentration, the better the resolution of higher molecular weight proteins.

Samples were loaded into wells in the gel. One lane is typically reserved for a marker (i.e., *ladder*), which is a mixture of proteins with defined molecular weights, usually stained so as to form visible, coloured bands; a single-colour (blue) ladder of GRISP was used.

When voltage was applied along the gel, proteins migrated into it at different speeds. These different rates of progression (different electrophoresis mobilities) separated sample proteins in bands, within each lane.

### **3.3.2.3 Transfer**

To make the proteins accessible to antibody detection, they were moved from within the gel onto a polyvinylidene difluoride (PVDF) membrane through electroblotting, in semi-dry conditions, using a Trans-blot® Turbo™ Blotting System (Bio-Rad, CA, USA), for 30 min, at 100V. The method uses the electric current to pull proteins from the gel into the PVDF membrane, maintaining the organisation they had within the gel.

### **3.3.2.4 Membrane blocking**

Membrane blocking is an important process that prevents interactions between nonspecific bonds of the membrane with the antibody used for detection of the target protein. This process is achieved by placing the membrane in a 3-5% bovine serum albumin (BSA) solution or non-fat dry milk, diluted in Tris-buffered saline (TBS; consisting of 0.2 M Trizma Base and 1.37 M NaCl) with a minute percentage of detergent such as Tween 20 or Triton X-100.

Membranes were blocked in 5% skimmed milk/ 0.1% Tween 20 prepared in TBS (TBST, pH 7.6), for 2 h at room temperature, in an orbital shaker, and then washed with TBST, three times, for 10 min each.

### **3.3.2.5 Detection**

During the detection the membrane is “probed” for the protein of interest with a modified antibody.

#### *3.3.2.5.1 Primary antibody*

Primary antibodies are generated when a host species or immune cell culture is exposed to the protein of interest (or a part thereof).

After blocking, the membrane is incubated with a diluted primary antibody solution (between 0.5 and 5 µg/mL), under gentle agitation, overnight. Usually, the solution is composed of buffered saline solution with a small percentage of detergent and sometimes with powdered milk or BSA.

The membranes were incubated overnight, at 4°C, with the following primary antibodies: mouse anti-ATG5 (1:1000, Biolegend, San Diego, CA, USA), mouse anti-Beclin-1 (1:1000, Biolegend, San Diego, CA USA), mouse anti-LC3 (1:1000, Biolegend, San Diego, CA USA), rat anti-Rab7a (1:1000, Biolegend, San Diego, CA, USA) and mouse anti-ubiquitin (1:100, Biolegend, San Diego, CA USA). Blots were also probed for mouse anti-β-actin (1:5,000, Sigma-Aldrich, St Louis, MO, USA) to ascertain equal sample loading. Primary antibodies were diluted in 1% BSA prepared in TBST, supplemented 0.05% sodium

azide. Sodium azide was used to conserve and reuse the primary antibody solutions. The membranes were then washed in TBST three times, for 10 min each, to remove unbound primary antibody.

#### 3.3.2.5.2 Secondary antibody

After rinsing with TBST, the membrane was exposed to a secondary antibody, directed at a species-species portion of the primary antibody. Antibodies come from animal sources; an anti-mouse secondary antibody will bind to almost any mouse-sourced primary antibody. Several secondary antibodies will bind to one primary antibody, enhancing the detection signal. The secondary antibody is typically linked to biotin or to a reporter enzyme such as alkaline phosphatase or horseradish peroxidase.

In this case, a secondary antibody linked to horseradish peroxidase was used, with 1% BSA diluted in TBST. The membrane was incubated for 1 h, at room temperature, under stirring with the horseradish peroxidase-conjugated goat anti-mouse immunoglobulin (IgG, 1:20,000, Advansta, CA, USA) and the horseradish peroxidase-conjugated goat anti-rat immunoglobulin (1:20,000, Advansta, CA, USA) and then washed in TBST (three washes for 10 min each).

#### 3.3.2.6 Chemiluminescent detection

Protein bands were detected by incubating the membranes in Clarity Western ECL Substrate (Bio-Rad, Hercules, CA, USA) for 5 min. The membranes were then imaged using the molecular imager ChemiDoc™ XRS (Bio-Rad, Hercules, CA, USA).

#### 3.3.2.7 Stripping

The stripping was performed with 10 mL of stripping solution (GRiSP Research Solutions, Porto, Portugal), for 5 min. at room temperature, using an orbital shaker. After stripping, membrane was 3x washed with TBST and then blocked, allowing membranes “reprobing” with loading control (*i.e.*, anti- $\beta$ -actin). In cases where it was required to assess the expression of a second protein in a previously developed membrane, this stripping process allowed the removal of the antibody previously used in the membrane, so that it is



possible to repeat the incubation process again with a new primary antibody. It is a process that must be carried out before membrane storage, at -20°C.

### **3.4 Statistical analysis**

Band intensities in each membrane lane were quantified using the Bio-Rad Image Lab (Version 5.1, Build 7, Bio-Rad, Hercules, CA, USA) and normalised against the intensity of  $\beta$ -actin (the housekeeping control). Results were expressed as mean  $\pm$  SD of the fold-change relative to the control. Statistical analysis was performed using GraphPad Prism 7 Software (GraphPad Software, La Jolla, CA). Analysis of the distribution normality was assessed using the Shapiro–Wilk and Kolmogorov-Smirnov normality tests, taking into account the acceptability of skewness and kurtosis values. Based on the normality results, one-way ANOVA, followed by a Dunnett's multiple comparisons test were performed, as appropriate.

## 4. RESULTS AND DISCUSSION

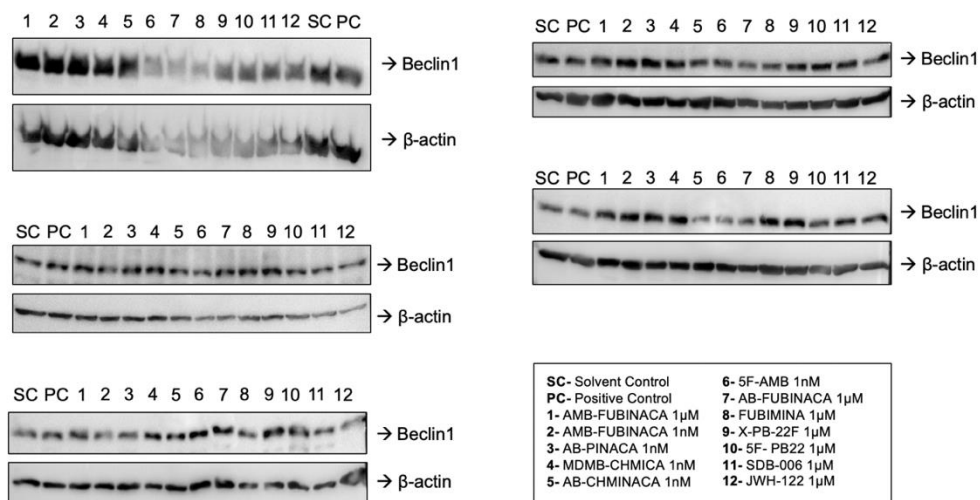
### 4.1 Alterations on autophagic mediators

To elucidate the mechanisms involved in the SC-induced activation of autophagy, NG108-15 cells were exposed to SCs for 24 hours, and protein expression of Beclin-1, ATG5, LC3, Rab7A, and ubiquitin, was analyzed.

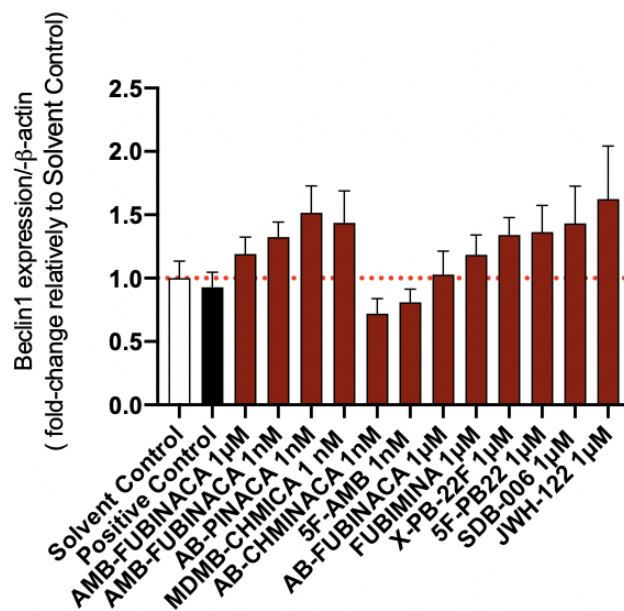
Of note, in this study, starvation medium was used as a positive control, as it had been previously referred in the literature as an autophagic stimulus that triggers cytoprotective autophagy [47]. However, as observed in all graphs (Fig. 5B, 6B, 7B and 8B), this stimulus did not work as a proper positive control, failing to validate the assays, and, unfortunately, in view of the short time available, it was not possible to test another positive control.

#### 4.1.1 Alterations on autophagic mediator Beclin-1

In the results for the autophagy marker Beclin-1, it can be seen that the expression of Beclin-1 following exposure to all of the tested SCs, except AB-CHMINACA and 5F-AMB, were above the control (**Fig. 5**). However, these changes were not statistically significant.



A



B

**Figure 5.** Expression of autophagic intermediary Beclin-1, in response to SCs, as assessed by Western-Blot.

In contrast, Casarejos et al. (2013) demonstrated that the treatment with 1mL/Kg of Sativex<sup>®</sup> (a mixture of  $\Delta^9$ -THC and CBD), every day for a month in parkin-null, human tau overexpressing ( $PK^{-/-}/Tau^{VLW}$ ) mice, a model of complex frontotemporal dementia, parkinsonism, and lower motor neuron disease, led to an increased turnover of LC3-I to LC3-II and increased levels of Beclin-1, assessed by immunoblotting. Based on these data, the authors concluded that Sativex<sup>®</sup> induced autophagy in  $PK^{-/-}/Tau^{VLW}$  mice [48].

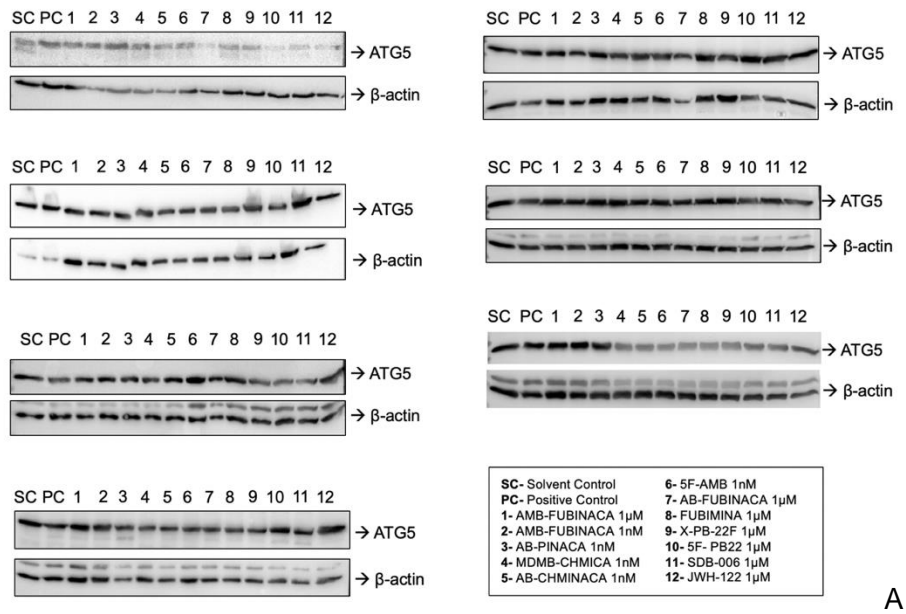
Shrivastava et al. (2011) found that the treatment with 10  $\mu\text{mol/L}$  CBD for 24h in MDA-MB-231 breast cancer cells, increased cleaved Beclin-1 and also, the treatment with 7.5  $\mu\text{mol/L}$  of CBD for 16h in the same cell line increases LC3-II levels, representing the induction of autophagy [49]. Moreover, Nabissi et al. (2015) also found that treatment with 10  $\mu\text{M}$  of CBD for 24h, in glioma stem-like cells, increases the cleaved LC3-II form levels and the protein Beclin-1, proving CBD-induced autophagy [50]. In agreement with these findings, Lin et al. (2020) observed that treatment of a rat model of hemorrhagic shock with 5 mg/Kg CBD increased LC3-II and Beclin-1 expression, indicating the activation of autophagy [51].

Pellerito et al. (2014) found that the treatment of human colon cancer HT29, HCT116 and Caco-2 cell lines with 10  $\mu\text{M}$  WIN55,212-2 did not modify Beclin-1 expression up to 36h. To further exclude an involvement of Beclin-1 in WIN55,212-2-mediated action, the authors performed RNAi-mediated silencing of Beclin-1 in HT29 cells. Beclin-1 knockdown was ineffective both on LC3-II accumulation and on WIN cytotoxic effect suggesting that WIN55,212-2 induced a Beclin-1-independent autophagic pathway [46].

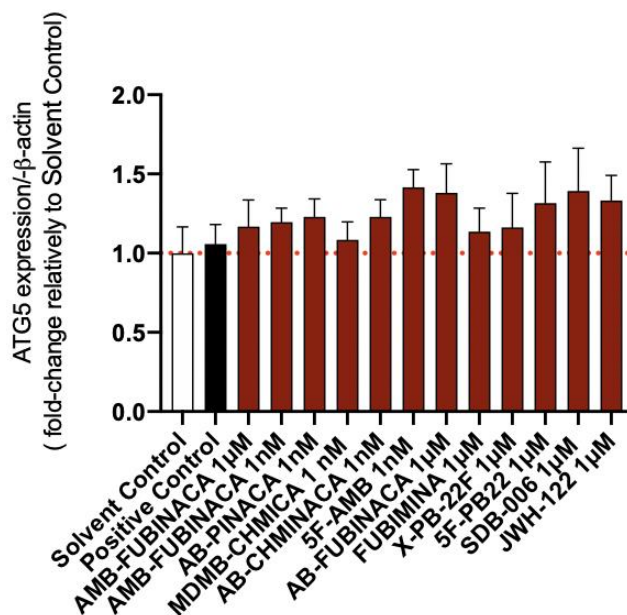
Notaro et al. (2014) reported that the treatment of human osteosarcoma MG63 cells with 5 $\mu\text{M}$  WIN55,212-2, produced no alterations in the marker for autophagosome formation, Beclin-1 [52].

#### **4.1.2 Alterations on autophagic mediator ATG5**

All SCs increased the autophagic related gene, ATG5, over the control (**Fig. 6**), although no statistically significant differences were observed either.



A



B

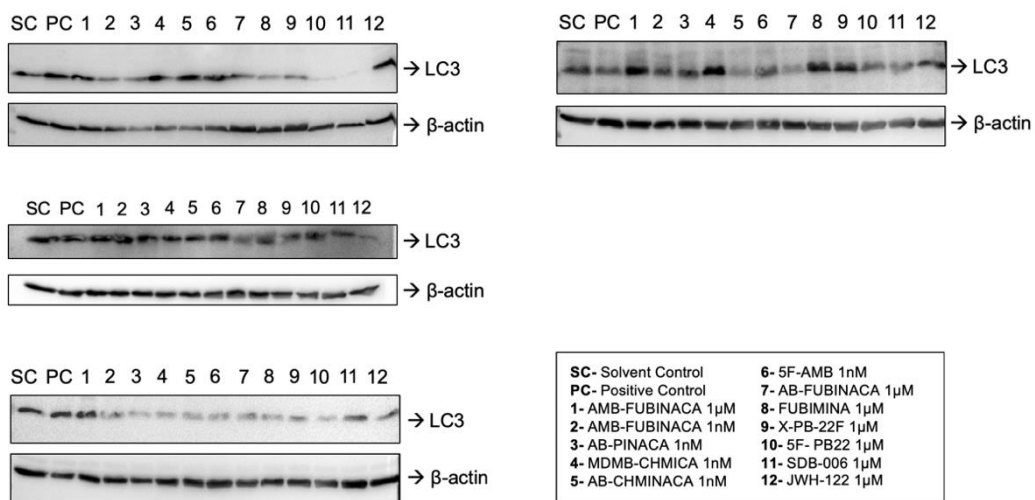
**Figure 6.** Expression of autophagic intermediary ATG5, in response to SCs, as assessed by Western-Blot.

Liu et al. (2020) showed that the treatment of PC12 rat pheochromocytoma cells with N-linoleylytyrosine (NITyr), an SC analogue of AEA, was found to upregulate the protein expression levels of LC3, Beclin-1 and ATG5, indicating that this SC induced autophagy in

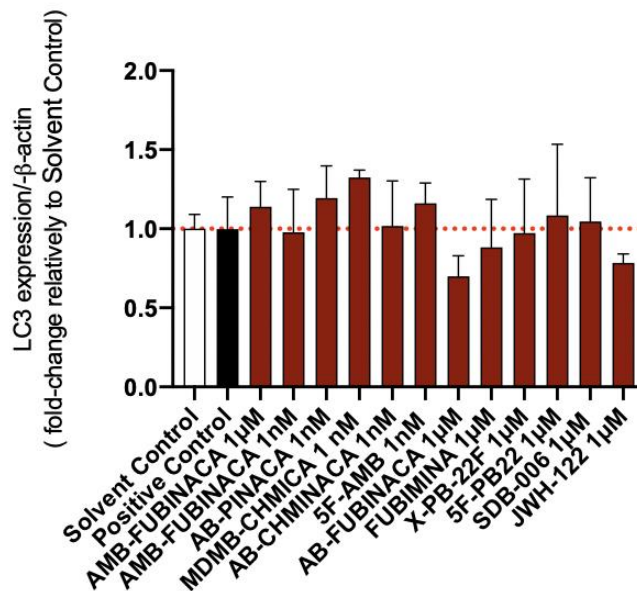
that cell line [53]. It was the first study, according to our knowledge, using ATG5 as a marker for cannabinoid-induced autophagy.

### 4.1.3 Alterations on autophagic mediator LC3

As its molecular weight is extremely low (14.7 kDa), LC3 is a difficult antibody to label. Nevertheless, its expression was increased in the presence of all SCs, except AMB-FUBINACA (1 nM), AB-FUBINACA (1  $\mu$ M), FUBIMINA (1  $\mu$ M), X-PB-22F (1  $\mu$ M), and JWH-



A



B

**Figure 7.** Expression of autophagic intermediary LC3, in response to SCs, as assessed by Western-Blot

122 (1  $\mu\text{M}$ ) (**Fig. 7**). However, once again it was not possible to observe statistically significant differences between SCs and the control. The reduced number of samples could most likely explain the absence of statistical differences.

The most widely used approaches in autophagy research are those using LC3 as an autophagy marker due to its specificity in labeling autophagosomes. Nonetheless, its sensitivity varies depending on the cell type or drug exposure settings that induce autophagy [6].

López-Valero et al. (2018) showed that treatment with 15 mg/Kg of  $\Delta^9$ -THC in mice injected with human brain U87MG cell line increased LC3 levels, determined by Western-blot, proving autophagy. Also, the combination of Sativex-like (10.5 mg/Kg of THC and 10 mg/Kg of CBD) and alkylating agent temozolomide produced a further increase in autophagy, determined by LC3 immunostaining, as compared with the individual treatments [54].

Koay et al. (2014) determined that the treatment with 10 $\mu\text{M}$  of CBD, within 4-6 h, in fully differentiated Caco-2 cells (a model of mature intestinal epithelium) increased LC3-II levels, and this effect was dose-dependent once there were tested concentrations from 0.1 to 25  $\mu\text{M}$  for 4 h and only 10 $\mu\text{M}$  and 25 $\mu\text{M}$  of CBD were able to increase LC3-II levels. It was also shown that the treatment with 100 nM ACEA and 10  $\mu\text{M}$  arachidonoyl cyclopropamide (AEA), for 4 h, in the same cell line, significantly increased LC3-II formation, in a dose-dependent manner since such effects were only observed for the higher concentrations tested (i.e., 100 nM ACEA and 10  $\mu\text{M}$  AEA). So, they found that all three types of cannabinoids, i.e., phytocannabinoids (e.g., CBD), endocannabinoids (e.g., AEA), and SCs (e.g., ACEA), significantly enhanced LC3-II formation in a dose-dependent manner. Notably, CBD was the only one that did not require CB1R to induce autophagy, as ACEA and AEA induced canonical autophagy, which is CB1R-mediated [55]. Moreover, Donadelli et al. (2011) showed that the treatment with 40  $\mu\text{M}$  GW405833 (an SC), 225  $\mu\text{M}$  arachidonoyl cyclopropamide (ACPA, an SC) and 40  $\mu\text{M}$  SR141716 (rimonabant, a CB1R selective antagonist) for 24h, in pancreatic adenocarcinoma cells, increased LC3 levels, proving cannabinoid-induced autophagy [2].

Armstrong et al. (2015) observed that the treatment of three human melanoma cell lines (CHL-1, A375, and SK-MEL-28) with 4.5  $\mu\text{M}$  or 5  $\mu\text{M}$   $\Delta^9$ -THC, for 24h increased LC3-II induction, and further increased in the presence of 10  $\mu\text{M}$  of chloroquine for the final 2h, demonstrating that  $\Delta^9$ -THC activates autophagy in melanoma cells [56]. In agreement, Lorente et al. (2011) found that  $\Delta^9$ -THC-induced autophagy in human glioma T98 and HG2 cells was enhanced by Knockdown of growth factor midkine (Mdk) or anaplastic lymphoma kinase (ALK). This was determined following the identification of the presence of cells with LC3 dots, as well as by the accumulation of the lipidated form of LC3 (LC3-II) [57]. Murase et al. (2014) showed that the treatment with 1.5  $\mu\text{M}$  of O-1663 ( $\Delta^9$ -THC analogue) and 3  $\mu\text{M}$  of  $\Delta^9$ -THC, in human breast cancer MDA-MB231 cells, induced autophagy, proved by the increased LC3-II levels, assessed by Western-Blot analysis. It was, also, observed that O-1663 was as effective as  $\Delta^9$ -THC and more effective than CBD at up-regulating the autophagy marker LC3-II, once 1.5  $\mu\text{M}$  of CBD produced only a minor up-regulation on the marker [58].

Nabissi et al. (2016) exposed multiple myeloma U266 and RPMI8226 cell lines with 12.5  $\mu\text{M}$  CBD and 12.5  $\mu\text{M}$   $\Delta^9$ -THC alone and in combination, for 24h. They analyzed the conversion of the soluble form of LC3 (LC3-I) to the lipidated and autophagosome-associated form (LC3-II), and observed that CBD alone induced a slight increase in the LC3-II/LC3-I ratio,  $\Delta^9$ -THC had no effect, while the  $\Delta^9$ -THC-CBD combination strongly augmented the levels of the cleaved LC3-II form and the LC3-II/ LC3-I ratio, compared with single treatments, concluding that CBD and  $\Delta^9$ -THC-CBD combination induced autophagic-cell death in this cell line [59]. Also, Andradas et al. (2021) showed that the treatment with 5.5  $\mu\text{M}$  of CBD in D283 medulloblastoma cells and the treatment with 5  $\mu\text{M}$  of CBD in D425 medulloblastoma cells, for 24h increased the marker used as an indicator of autophagy - LC3-II. In contrast, the authors were not able to prove that THC increases LC3-II levels in this cell lines [60].

Bockman et al. (2020) revealed a concentration-dependent increase in autophagy marker LC3-II with the treatment with 3, 6 and 10  $\mu\text{M}$  of CBD, for 24h, in human umbilical vein endothelial cells, concluding that CBD induced a concentration-dependent increase in cellular autophagy [61]. After exposing adipose tissue-derived mesenchymal stem cells to different CBD concentrations (0.1, 1 and 3  $\mu\text{M}$ ) for 24h, Bublitz et al. (2020) showed that only the treatment with 3  $\mu\text{M}$  CBD increased the LC3-II expression, and that this concentration was time-dependent over a period of 6 to 48h. The authors also showed that



the treatment with 3  $\mu\text{M}$  of R(+)-methanandamide (an endocannabinoid), increased LC3-II, with a similar time-dependent effect. The authors thus concluded that both cannabinoids induced time- and concentration- dependent increases in the autophagy marker LC3-II [62].

Similarly, Vrechi et al. (2021) showed that 10 and 50  $\mu\text{M}$  CBD treatment increased LC3-II levels in SH-SY5Y cells, relatively to the control group. This result was potentiated by  $\text{NH}_4\text{Cl}$ , an inhibitor of lysosomal activity. Of note, the use of this inhibitor promoted the accumulation of “undigested” lipidated LC3-II and allowed to discriminate the increased autophagosome formation promoted only by the CBD treatment. In this way, the authors proved that the LC3-II formation was not due to autophagic inhibition but to an enhanced autophagy progression that could lead to faster LC3-II degradation, as observed in control cells. Moreover, the authors ascertained the involvement of CB1R, CB2R and TRPV1 receptor activation in CBD-induced autophagy noting that the increase in LC3-II levels promoted by the treatment with 10  $\mu\text{M}$  CBD, under blockade of  $\text{NH}_4\text{Cl}$  (added during the last hour of treatment), was reverted by 30 min pre-treatment of SH-SY5Y cells and murine astrocytes with 10  $\mu\text{M}$  of AM251 (a CB1R antagonist), AM630 (a CB2R antagonist) and capsazepine (a TRPV1 antagonist), in both cell lines, denoting the involvement of the activation of those receptors in CBD-induced autophagy. As such, the authors suggested that exposure to CBD could activate autophagy via the activation of canonical cannabinoid receptors [63].

Marinelli et al. (2020) showed an increase in LC3-II in human endometrial cancer (EC) PCEM004a cells, following 7.85  $\mu\text{g}/\text{mL}$  CBD treatment, for 48h and 72h and with 3.92  $\mu\text{g}/\text{mL}$  CBD treatment after 72h, concluding that CBD induced autophagy in this cell line [64]. Henry et al. (2021) demonstrated that the treatment of canine neoplastic cells with 10  $\mu\text{g}/\text{mL}$  CBD for 2 h induced autophagy, verified by the increase levels of LC3-II, which persisted through 8h [65]. Amaral et al. (2021) found that the treatment of estrogen receptor-positive breast cancer cells (MCF-7aro) stimulated with 1nM of testosterone with 10  $\mu\text{M}$  CBD significantly increased LC3-I/LC3-II expression ratio over control groups after 1 day of treatment, confirming the occurrence of CBD-induced autophagy in this cell line [66].

Vara et al. (2011) found that treatment with 8  $\mu\text{M}$   $\Delta^9$ -THC and 8  $\mu\text{M}$  JWH-015 (an SC) of human hepatocellular liver carcinoma HepG2 cell line and hepatocellular carcinoma HuH-7 cells induced autophagy, as indicated by increased LC3-II levels, measured by Western-Blot [42].

There are also reports of SCs altering LC3-II levels in different cell models. For example, Notaro et al. (2014) found that the treatment with 5  $\mu\text{M}$  WIN55,212-2 induced a time-dependent enhancement of LC3-II, after 16 h treatment in human osteosarcoma MG63 cells, concluding that WIN55,212-2 induce autophagic markers [52]. In contrast, Zhang et al. (2016) observed that treatment with 10, 20 and 30  $\mu\text{M}$  of WIN55,212-2, increased expression of the proteins LC3 and Beclin-1, indicating WIN55, 212-2-induced autophagy in osteosarcoma cell line SaOs-2 [5]. Pellerito et al. (2014) found that the treatment of human colon cancer HT29 HCT 116 and Caco-2 cell lines with 10  $\mu\text{M}$  of the same SC, for 36h, triggered an autophagic response characterized by the increase of the LC3 autophagy marker. In HT29 cells, the effects on LC3 were time-dependent, being already detectable at 8h of treatment. The authors concluded that WIN55,212-2 induced the autophagic process in colon cancer cells. [46].

Ellert-Miklaszewska et al. (2021) demonstrated that the treatment of in glioblastoma cell lines with the SCs WIN55,212-2 and JWH-133 for 12-48h, was associated with the induction of autophagy, evidenced by the increase of acidic vesicular organelles formation and processing of LC3, in a time-dependent manner, demonstrating that the treatment with SCs is associated with induction of autophagy. Treated cells were co-incubated with 10 nM of Bafilomycin A1, an autophagic inhibitor, for the last 4h to exclude that LC3-II increase was induced by lysosomal degradation [67].

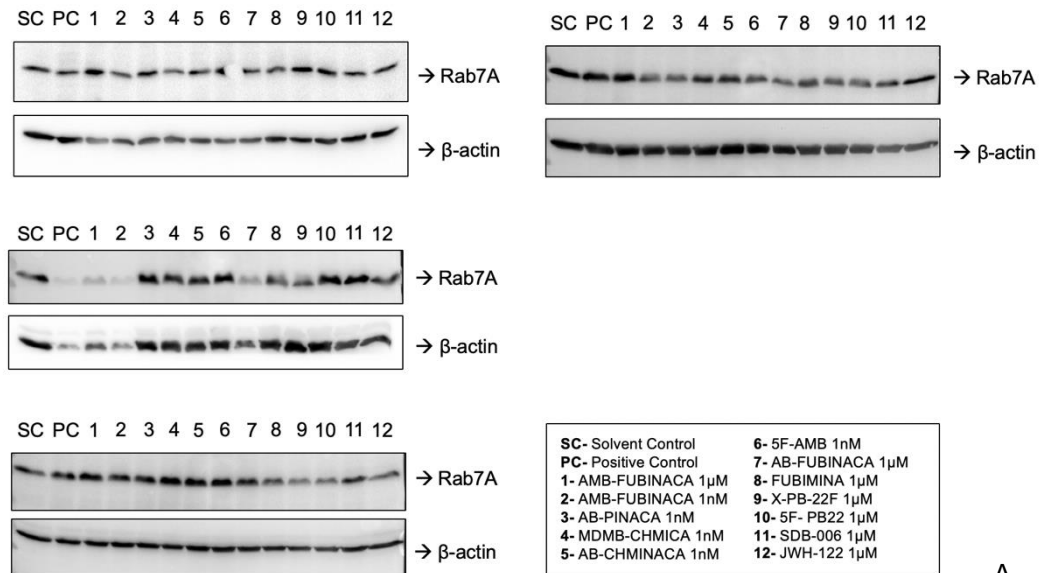
#### 4.1.4 Alterations on autophagic mediator Rab7A

Concerning the autophagy intermediary Rab7A, the results showed an increase only for AMB-FUBINACA (1  $\mu\text{M}$ ), AB-PINACA (1 nM), AB-CHMINACA (1 nM) and SDB-006 (1  $\mu\text{M}$ ) over control (**Fig. 8**). The results have no statistic significancy, which could be also attributed to the small number of samples.

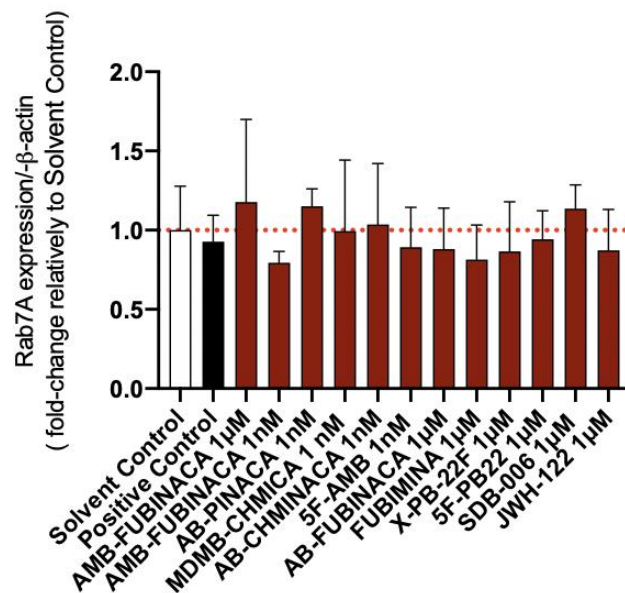
The small GTPase, Rab7A, was shown to have different roles in both endosomal membrane traffic and autophagy. For example, it plays a very important role in autophagy, since the autolysosome maturation and autophagosome fusion with the lysosome are attributed to the activity of this protein. In particular, silencing of Rab7A causes an accumulation of late autophagic vacuoles, indicating a need for Rab7a's activity in their

destruction by fusion with lysosomes [20, 21]. For those reasons, it was expected to see alterations on its expression.

Interestingly, to the best of our knowledge, the expression of Rab7A has never been evaluated after cannabinoids treatment for detection of autophagy.



A



B

**Figure 8.** Expression of autophagic intermediary Rab7A, in response to SCs, as assessed by Western-Blot

#### 4.1.5 Alterations on autophagic mediator ubiquitin

Despite the important role of ubiquitin in autophagy has been proved, in the present study, the antibody appears to have detected ubiquitin at different molecular weights (**Fig.9**), which could indicate the detection of ubiquitinated proteins, targeted for degradation, becoming difficult to establish an association between ubiquitin expression only related to autophagy. Of note, this was the first time, to the best of our knowledge, that this protein was used as marker for cannabinoid-induced autophagy. However, based on our findings, ubiquitin does not seem to be the most suitable marker for this purpose.

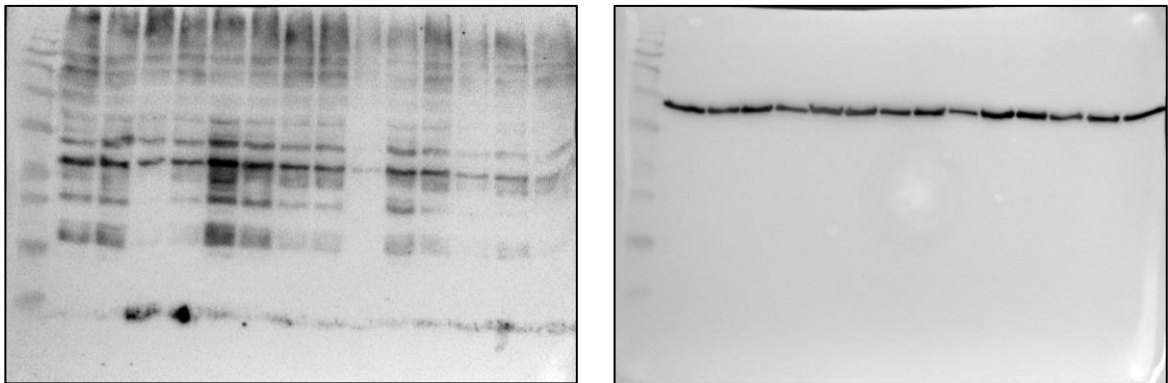


**Figure 9.** Expression of autophagic intermediary ubiquitin, in response to SCs, as assessed by Western-Blot.

So, although several reports have shown the increased expression of different autophagy markers following cannabinoid (phytocannabinoids, endocannabinoids or SCs) exposure, and despite the visible increase of SCs over control in our studies (Figs. 5B, 6B, 7B, 8B), we were not able to associate any modification in the expression of autophagic markers to SC-induced autophagy, most likely due to the high variability in the data obtained (**appendixes I, II, III and IV**) and the reduced number of independent experiments performed.

## 5. CONCLUSIONS

In conclusion, we were not able to ascertain the mechanisms involved in the SC-induced autophagy in NG108-15 cells, despite the visible increase in some SCs over control group. This could be attributed to different factors, including the high data variability, the reduced number of independent experiments (lower statistical power) or to the differences in the used methodology (e.g., we did not use potentiators of autophagy markers). Of note, this was the first study that tried to use Rab7A and ubiquitin as cannabinoid-induced autophagy markers.

We further queried the literature to ascertain the effects of cannabinoids in the induction of autophagy in other cell lines, noting that different cannabinoids may trigger this process, which in some cases, was found to be time- and concentration-dependent.

In addition, it should be noted that the Covid-19 pandemic-related lockdown prevented a more efficient optimization of the procedure for detection of the autophagic markers addressed in this study, due to the restricted access to the labs.

In this sense, to help to elucidate the toxicological effects of SCs and, in particular, to better understand how these substances increase autophagy, further research is required to peremptorily conclude on the involvement of ATG5, Beclin-1, LC3, Rab7A and ubiquitin on autophagy process.

## 6. REFERENCES

1. Glick, D., S. Barth, and K.F. Macleod, *Autophagy: cellular and molecular mechanisms*. J Pathol, 2010. **221**(1): p. 3-12.
2. Donadelli, M., et al., *Gemcitabine/cannabinoid combination triggers autophagy in pancreatic cancer cells through a ROS-mediated mechanism*. Cell Death Dis, 2011. **2**: p. e152.
3. Schoeman, R., N. Beukes, and C. Frost, *Cannabinoid Combination Induces Cytoplasmic Vacuolation in MCF-7 Breast Cancer Cells*. Molecules, 2020. **25**(20).
4. Dando, I., et al., *Cannabinoids inhibit energetic metabolism and induce AMPK-dependent autophagy in pancreatic cancer cells*. Cell Death Dis, 2013. **4**: p. e664.
5. Zhang, G., et al., *Inhibition of autophagy and enhancement of endoplasmic reticulum stress increase sensitivity of osteosarcoma Saos-2 cells to cannabinoid receptor agonist WIN55,212-2*. Cell Biochem Funct, 2016. **34**(5): p. 351-8.
6. Guo, S., et al., *A rapid and high content assay that measures cyto-ID-stained autophagic compartments and estimates autophagy flux with potential clinical applications*. Autophagy, 2015. **11**(3): p. 560-72.
7. Calvaruso, G., et al., *Cannabinoid-associated cell death mechanisms in tumor models (review)*. Int J Oncol, 2012. **41**(2): p. 407-13.
8. Majeski, A.E. and J.F. Dice, *Mechanisms of chaperone-mediated autophagy*. Int J Biochem Cell Biol, 2004. **36**(12): p. 2435-44.
9. Levine, B. and V. Deretic, *Unveiling the roles of autophagy in innate and adaptive immunity*. Nat Rev Immunol, 2007. **7**(10): p. 767-77.
10. Dikic, I. and Z. Elazar, *Mechanism and medical implications of mammalian autophagy*. Nat Rev Mol Cell Biol, 2018. **19**(6): p. 349-364.
11. Ichimiya, T., et al., *Autophagy and Autophagy-Related Diseases: A Review*. Int J Mol Sci, 2020. **21**(23).
12. Bar-Peled, L. and D.M. Sabatini, *Regulation of mTORC1 by amino acids*. Trends Cell Biol, 2014. **24**(7): p. 400-6.
13. Wang, Y. and H. Zhang, *Regulation of Autophagy by mTOR Signaling Pathway*. Adv Exp Med Biol, 2019. **1206**: p. 67-83.
14. Hosokawa, N., et al., *Nutrient-dependent mTORC1 association with the ULK1-Atg13-FIP200 complex required for autophagy*. Mol Biol Cell, 2009. **20**(7): p. 1981-91.

15. Pattingre, S., et al., *Bcl-2 antiapoptotic proteins inhibit Beclin 1-dependent autophagy*. Cell, 2005. **122**(6): p. 927-39.
16. Yin, Z., et al., *The Roles of Ubiquitin in Mediating Autophagy*. Cells, 2020. **9**(9).
17. Grumati, P. and I. Dikic, *Ubiquitin signaling and autophagy*. J Biol Chem, 2018. **293**(15): p. 5404-5413.
18. Brier, L.W., et al., *Regulation of LC3 lipidation by the autophagy-specific class III phosphatidylinositol-3 kinase complex*. Mol Biol Cell, 2019. **30**(9): p. 1098-1107.
19. Yoshimori, T., *Autophagy: a regulated bulk degradation process inside cells*. Biochem Biophys Res Commun, 2004. **313**(2): p. 453-8.
20. Hyttinen, J.M., et al., *Maturation of autophagosomes and endosomes: a key role for Rab7*. Biochim Biophys Acta, 2013. **1833**(3): p. 503-10.
21. Tan, E.H.N. and B.L. Tang, *Rab7a and Mitophagosome Formation*. Cells, 2019. **8**(3).
22. Lee, X.C., E. Werner, and M. Falasca, *Molecular Mechanism of Autophagy and Its Regulation by Cannabinoids in Cancer*. Cancers (Basel), 2021. **13**(6).
23. Wiley, J.L., R.A. Owens, and A.H. Lichtman, *Discriminative Stimulus Properties of Phytocannabinoids, Endocannabinoids, and Synthetic Cannabinoids*. Curr Top Behav Neurosci, 2018. **39**: p. 153-173.
24. Ko, G.D., et al., *Medical cannabis - the Canadian perspective*. J Pain Res, 2016. **9**: p. 735-744.
25. Pertwee, R.G., *The diverse CB1 and CB2 receptor pharmacology of three plant cannabinoids: delta9-tetrahydrocannabinol, cannabidiol and delta9-tetrahydrocannabivarin*. Br J Pharmacol, 2008. **153**(2): p. 199-215.
26. Kataoka, K., et al., *Age-dependent Alteration in Mitochondrial Dynamics and Autophagy in Hippocampal Neuron of Cannabinoid CB1 Receptor-deficient Mice*. Brain Res Bull, 2020. **160**: p. 40-49.
27. du Plessis, S.S., A. Agarwal, and A. Syriac, *Marijuana, phytocannabinoids, the endocannabinoid system, and male fertility*. J Assist Reprod Genet, 2015. **32**(11): p. 1575-88.
28. Cristino, L., T. Bisogno, and V. Di Marzo, *Cannabinoids and the expanded endocannabinoid system in neurological disorders*. Nat Rev Neurol, 2020. **16**(1): p. 9-29.
29. Publications, U.N., *World Drug Report*. 2021, United Nations Office on Drugs and Crime p. 3-121.

30. Bilici, R., *Synthetic cannabinoids*. North Clin Istanb, 2014. **1**(2): p. 121-126.
31. Alves, V.L., et al., *The synthetic cannabinoids phenomenon: from structure to toxicological properties. A review*. Crit Rev Toxicol, 2020. **50**(5): p. 359-382.
32. Auwärter, V.d.M., J.; Gallegos, A.; Evans-Brown, M.; Rachel Christie, R.; Jorge, R. and Sedefov, R. , *Synthetic cannabinoids in Europe - a review 2021*, European Monitoring Centre for Drugs and Drug Addiction: Luxembourg: Publications Office of the European Union. p. 4-126.
33. Wells, D.L. and C.A. Ott, *The "new" marijuana*. Ann Pharmacother, 2011. **45**(3): p. 414-7.
34. Jerry, J., G. Collins, and D. Stroom, *Synthetic legal intoxicating drugs: the emerging 'incense' and 'bath salt' phenomenon*. Cleve Clin J Med, 2012. **79**(4): p. 258-64.
35. Le Boisselier, R., et al., *Focus on cannabinoids and synthetic cannabinoids*. Clin Pharmacol Ther, 2017. **101**(2): p. 220-229.
36. Shanks, K.G., et al., *Case reports of synthetic cannabinoid XLR-11 associated fatalities*. Forensic Sci Int, 2015. **252**: p. e6-9.
37. Hoyte, C.O., et al., *A characterization of synthetic cannabinoid exposures reported to the National Poison Data System in 2010*. Ann Emerg Med, 2012. **60**(4): p. 435-8.
38. Courts, J., et al., *Signs and symptoms associated with synthetic cannabinoid toxicity: systematic review*. Australas Psychiatry, 2016. **24**(6): p. 598-601.
39. Kronstrand, R., et al., *Fatal Poisonings Associated with New Psychoactive Substances*. Handb Exp Pharmacol, 2018. **252**: p. 495-541.
40. Armenian, P., et al., *Intoxication from the novel synthetic cannabinoids AB-PINACA and ADB-PINACA: A case series and review of the literature*. Neuropharmacology, 2018. **134**(Pt A): p. 82-91.
41. Salazar, M., et al., *Cannabinoid action induces autophagy-mediated cell death through stimulation of ER stress in human glioma cells*. J Clin Invest, 2009. **119**(5): p. 1359-72.
42. Vara, D., et al., *Anti-tumoral action of cannabinoids on hepatocellular carcinoma: role of AMPK-dependent activation of autophagy*. Cell Death Differ, 2011. **18**(7): p. 1099-111.
43. Anderson, C.M. and K.F. Macleod, *Autophagy and cancer cell metabolism*. Int Rev Cell Mol Biol, 2019. **347**: p. 145-190.

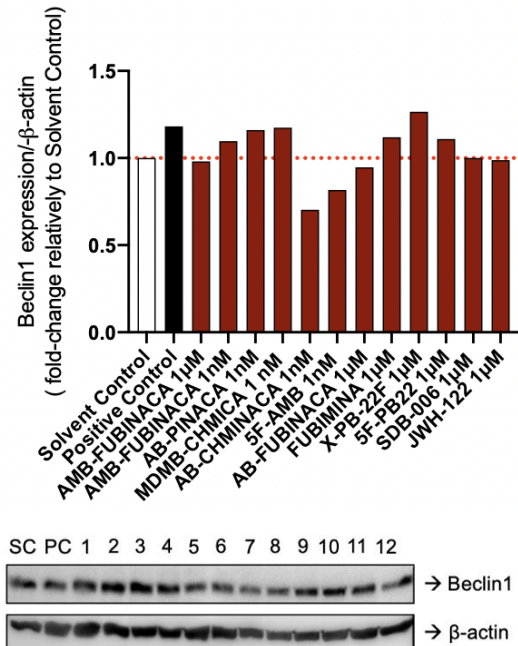
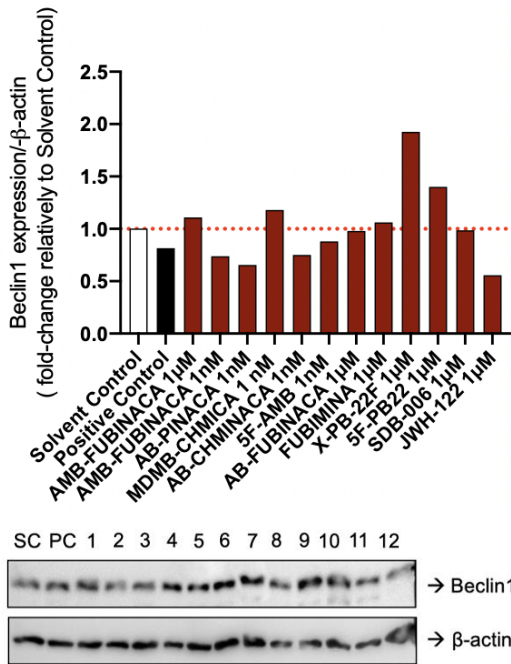
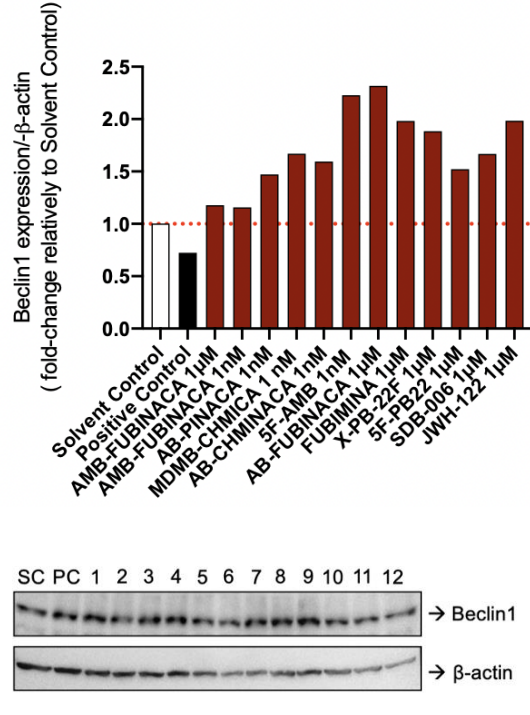
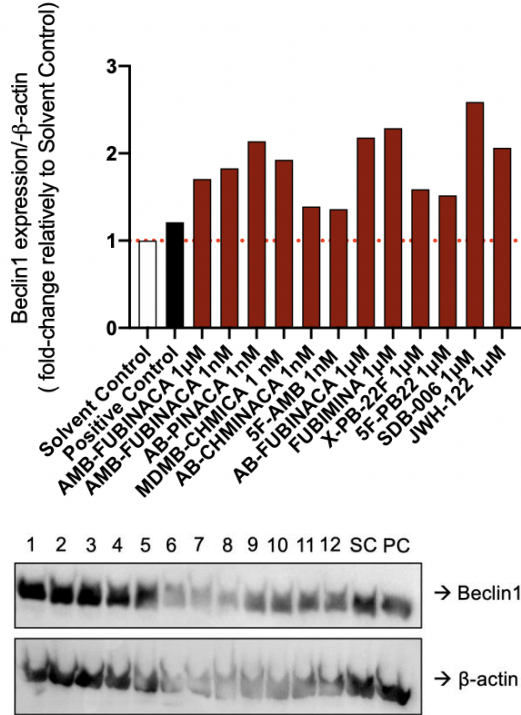


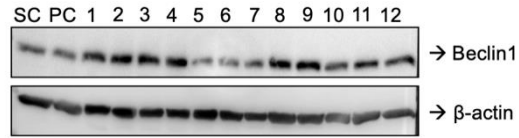
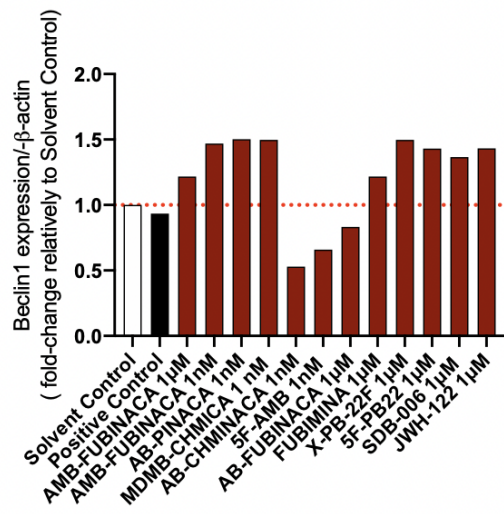
44. B'Chir, W., et al., *Dual role for CHOP in the crosstalk between autophagy and apoptosis to determine cell fate in response to amino acid deprivation*. Cell Signal, 2014. **26**(7): p. 1385-91.
45. Carracedo, A., et al., *The stress-regulated protein p8 mediates cannabinoid-induced apoptosis of tumor cells*. Cancer Cell, 2006. **9**(4): p. 301-12.
46. Pellerito, O., et al., *WIN induces apoptotic cell death in human colon cancer cells through a block of autophagic flux dependent on PPARgamma down-regulation*. Apoptosis, 2014. **19**(6): p. 1029-42.
47. Hernandez-Tiedra, S., et al., *Dihydroceramide accumulation mediates cytotoxic autophagy of cancer cells via autolysosome destabilization*. Autophagy, 2016. **12**(11): p. 2213-2229.
48. Casarejos, M.J., et al., *Natural cannabinoids improve dopamine neurotransmission and tau and amyloid pathology in a mouse model of tauopathy*. J Alzheimers Dis, 2013. **35**(3): p. 525-39.
49. Shrivastava, A., et al., *Cannabidiol induces programmed cell death in breast cancer cells by coordinating the cross-talk between apoptosis and autophagy*. Mol Cancer Ther, 2011. **10**(7): p. 1161-72.
50. Nabissi, M., et al., *Cannabidiol stimulates Aml-1a-dependent glial differentiation and inhibits glioma stem-like cells proliferation by inducing autophagy in a TRPV2-dependent manner*. Int J Cancer, 2015. **137**(8): p. 1855-69.
51. Lin, B., et al., *Cannabidiol alleviates hemorrhagic shock-induced neural apoptosis in rats by inducing autophagy through activation of the PI3K/AKT pathway*. Fundam Clin Pharmacol, 2020. **34**(6): p. 640-649.
52. Notaro, A., et al., *Involvement of PAR-4 in cannabinoid-dependent sensitization of osteosarcoma cells to TRAIL-induced apoptosis*. Int J Biol Sci, 2014. **10**(5): p. 466-78.
53. Liu, X., et al., *Nlinoleytyrosine protects PC12 cells against oxidative damage via autophagy: Possible involvement of CB1 receptor regulation*. Int J Mol Med, 2020. **46**(5): p. 1827-1837.
54. Lopez-Valero, I., et al., *Optimization of a preclinical therapy of cannabinoids in combination with temozolomide against glioma*. Biochem Pharmacol, 2018. **157**: p. 275-284.

55. Koay, L.C., R.J. Rigby, and K.L. Wright, *Cannabinoid-induced autophagy regulates suppressor of cytokine signaling-3 in intestinal epithelium*. *Am J Physiol Gastrointest Liver Physiol*, 2014. **307**(2): p. G140-8.
56. Armstrong, J.L., et al., *Exploiting cannabinoid-induced cytotoxic autophagy to drive melanoma cell death*. *J Invest Dermatol*, 2015. **135**(6): p. 1629-1637.
57. Lorente, M., et al., *Stimulation of the midkine/ALK axis renders glioma cells resistant to cannabinoid antitumoral action*. *Cell Death Differ*, 2011. **18**(6): p. 959-73.
58. Murase, R., et al., *Targeting multiple cannabinoid anti-tumour pathways with a resorcinol derivative leads to inhibition of advanced stages of breast cancer*. *Br J Pharmacol*, 2014. **171**(19): p. 4464-77.
59. Nabissi, M., et al., *Cannabinoids synergize with carfilzomib, reducing multiple myeloma cells viability and migration*. *Oncotarget*, 2016. **7**(47): p. 77543-77557.
60. Andradas, C., et al., *Assessment of Cannabidiol and Delta9-Tetrahydrocannabinol in Mouse Models of Medulloblastoma and Ependymoma*. *Cancers (Basel)*, 2021. **13**(2).
61. Bockmann, S. and B. Hinz, *Cannabidiol Promotes Endothelial Cell Survival by Heme Oxygenase-1-Mediated Autophagy*. *Cells*, 2020. **9**(7).
62. Bublitz, K., et al., *Cannabinoid-Induced Autophagy and Heme Oxygenase-1 Determine the Fate of Adipose Tissue-Derived Mesenchymal Stem Cells under Stressful Conditions*. *Cells*, 2020. **9**(10).
63. Vrechi, T.A.M., et al., *Cannabidiol induces autophagy via ERK1/2 activation in neural cells*. *Sci Rep*, 2021. **11**(1): p. 5434.
64. Marinelli, O., et al., *The Effects of Cannabidiol and Prognostic Role of TRPV2 in Human Endometrial Cancer*. *Int J Mol Sci*, 2020. **21**(15).
65. Henry, J.G., et al., *The effect of cannabidiol on canine neoplastic cell proliferation and mitogen-activated protein kinase activation during autophagy and apoptosis*. *Vet Comp Oncol*, 2021. **19**(2): p. 253-265.
66. Amaral, C., et al., *Unveiling the mechanism of action behind the anti-cancer properties of cannabinoids in ER(+) breast cancer cells: Impact on aromatase and steroid receptors*. *J Steroid Biochem Mol Biol*, 2021. **210**: p. 105876.
67. Ellert-Miklaszewska, A., I.A. Ciechomska, and B. Kaminska, *Synthetic Cannabinoids Induce Autophagy and Mitochondrial Apoptotic Pathways in Human Glioblastoma Cells Independently of Deficiency in TP53 or PTEN Tumor Suppressors*. *Cancers (Basel)*, 2021. **13**(3).

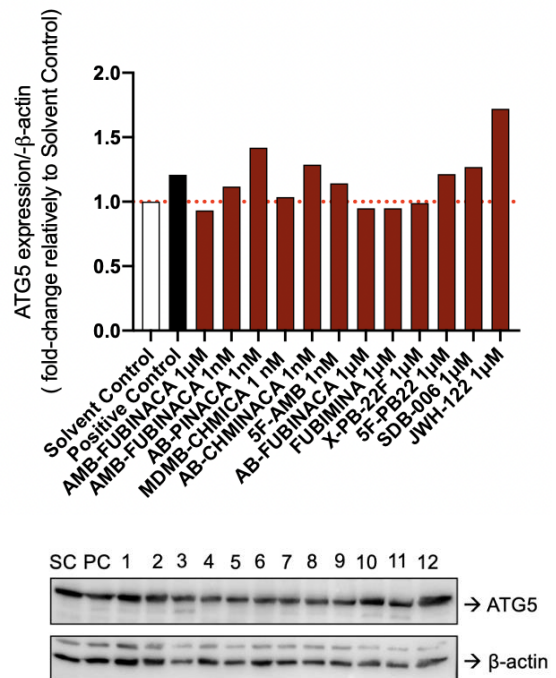
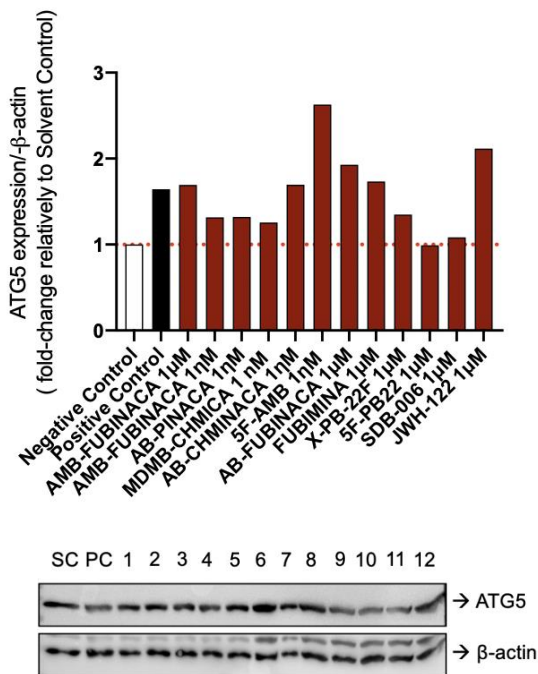
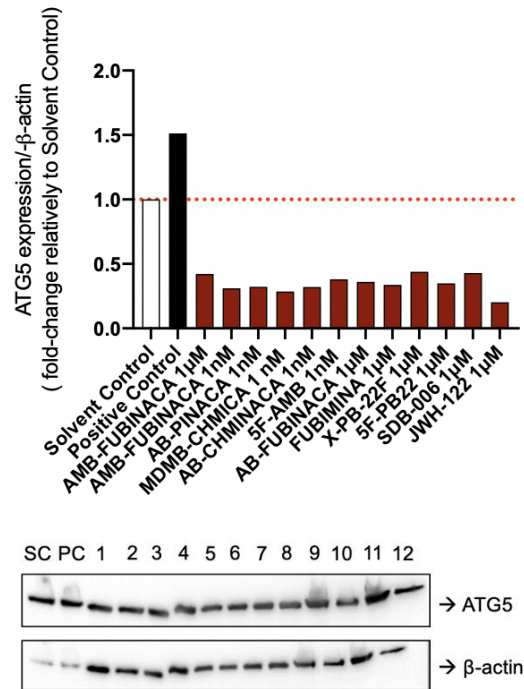
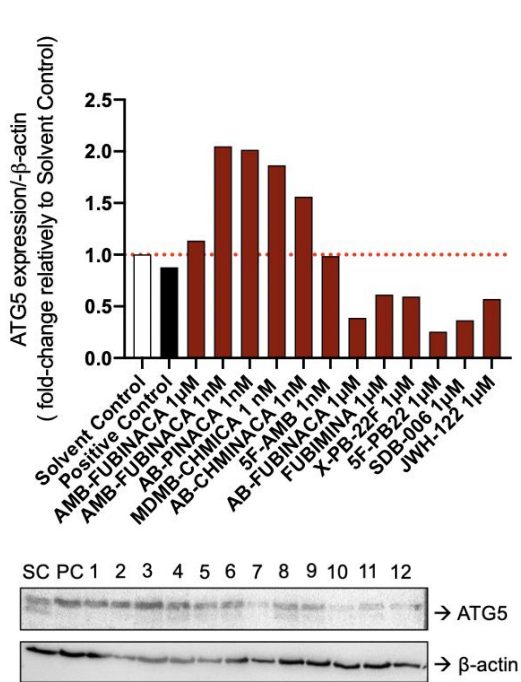
## 7. APPENDIXES

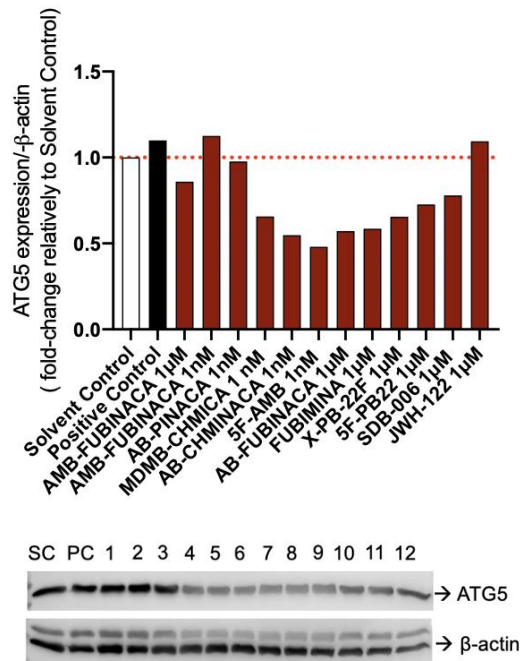
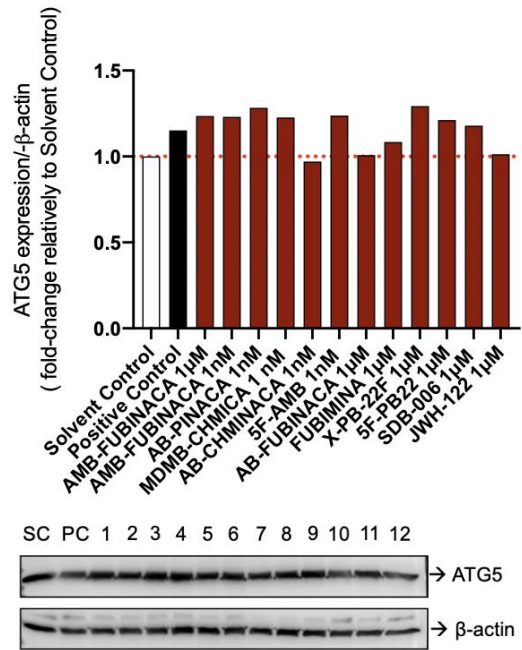
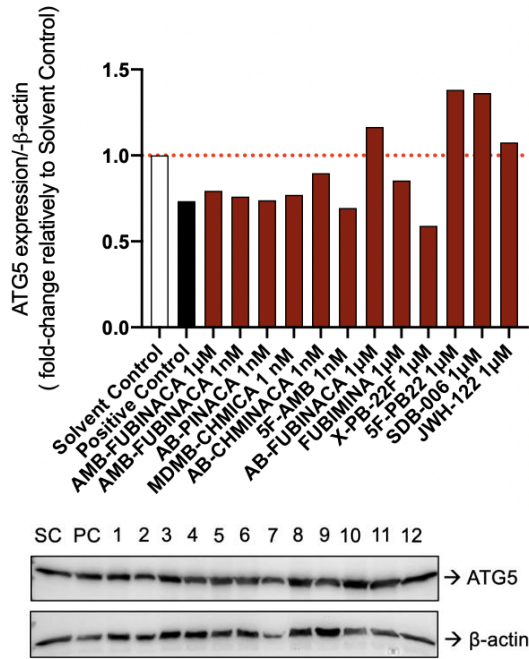
### I. Graphs of the different experiences for Beclin-1



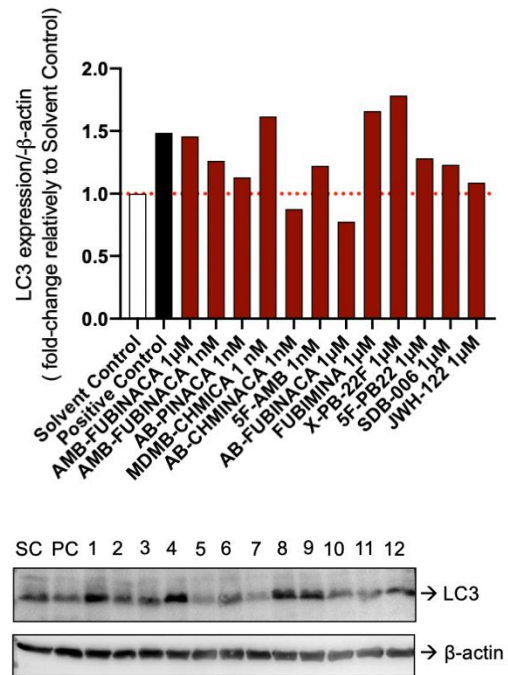
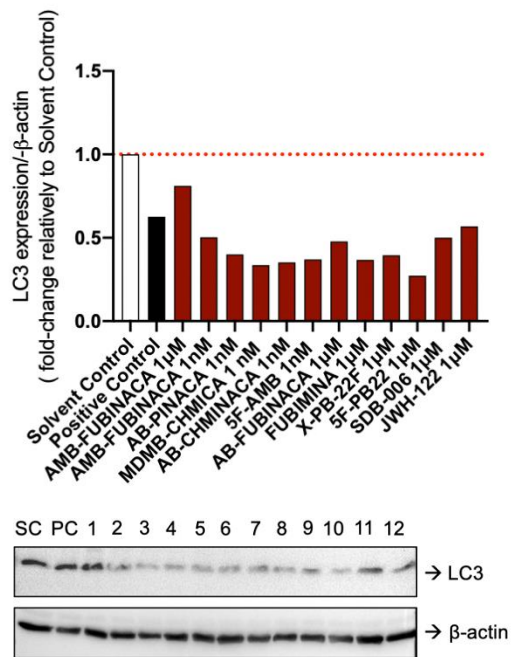
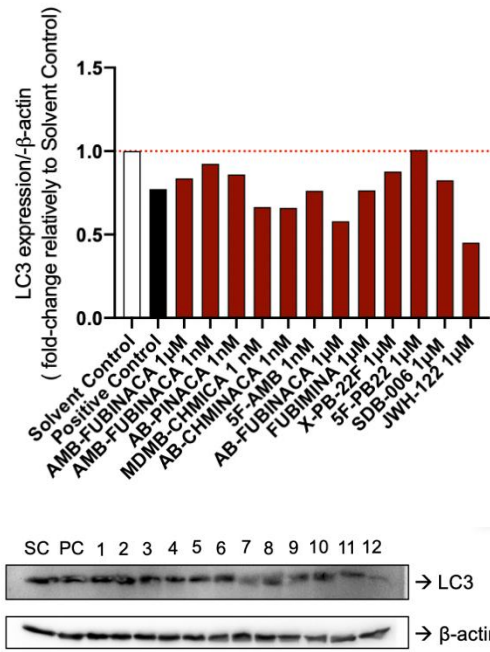
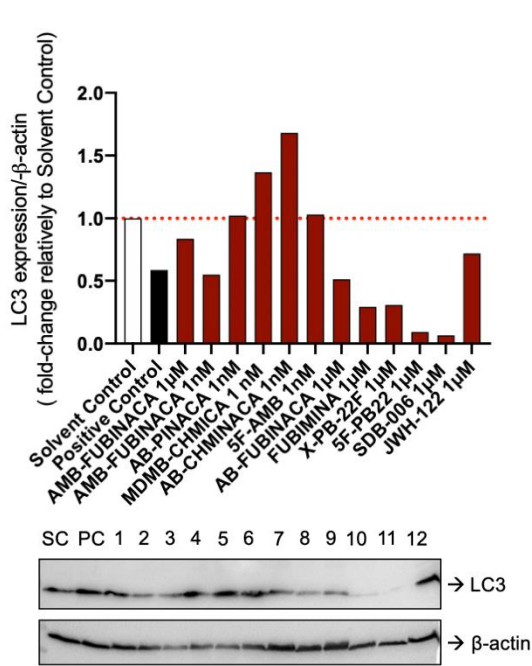


## II. Graphs of the different experiences for ATG5





### III. Graphs of the different experiences for LC3



#### IV. Graphs of the different experiences for Rab7A

